

Hydrologic Components for Model Development

By Carma A. San Juan, Wayne R. Belcher, Randell J. Laczniak, and Heather M. Putnam

Chapter C of

Death Valley Regional Ground-Water Flow System, Nevada and California—Hydrogeologic Framework and Transient Ground-Water Flow Model

Edited by Wayne R. Belcher

Prepared in cooperation with the
U.S. Department of Energy
Office of Environmental Management, National Nuclear Security Administration, Nevada Site Office,
under Interagency Agreement DE-AI52-01NV13944, and
Office of Repository Development,
under Interagency Agreement DE-AI08-02RW12167

Scientific Investigations Report 2004-5205

U.S. Department of the Interior
U.S. Geological Survey

Contents

Introduction	103
Water Budget	103
Ground-Water Discharge	103
Natural Ground-Water Discharge	105
Evapotranspiration	105
Springs.....	108
Staininger and Grapevine Springs.....	108
Texas, Travertine, and Nevares Springs.....	108
Indian and Cactus Springs.....	109
Bennetts and Manse Springs.....	109
Pumpage	110
Ground-Water Recharge	115
Lateral Flow.....	118
Balance of Components	118
Hydraulic Properties	120
Hydraulic Conductivity.....	120
Probability Distributions	121
Depth Decay	121
Hydraulic Head	122
Head Observations	122
Head-Observation Uncertainty	128
Well-Altitude Error	128
Well-Location Error	128
Nonsimulated Transient Error	130
Measurement Error	130
Total Head-Observation Error	130
Summary	132
References Cited	133

Figures

C-1. Map showing major areas of ground-water recharge, natural discharge, and pumpage, and model boundary segments of lateral flow in the Death Valley regional ground-water flow system region.....	104
C-2. Map showing major areas of natural ground-water discharge in the Death Valley regional ground-water flow system model domain.....	106
C-3. Graph showing annual discharge from regional springs in Pahrump Valley, Bennetts and Manse Springs, 1875–1978.....	110
C-4. Map showing spatial distribution of pumping wells by water-use class and total pumpage for 1913–98 by hydrographic area.....	111
C-5. Graph showing annual ground-water pumpage estimates developed by water-use class from Death Valley regional ground-water flow system model domain, 1913–98.....	113
C-6. Graph of uncertainty in annual ground-water pumpage estimates developed for Death Valley regional ground-water flow system model domain, 1913–98	114

C-7—C-9.	Maps showing:	
C-7.	Simulated average annual precipitation and stream-gaging stations used to calibrate the net-infiltration model in the Death Valley regional ground-water flow system model region	116
C-8.	Simulated net infiltration used to estimate recharge to the Death Valley regional ground-water flow system model region, 1950–99	117
C-9.	Regional ground-water potentiometric surface and lateral flow across boundary segments of the Death Valley regional ground-water flow model domain	119
C-10.	Annotated hydrograph showing general- and detailed-condition attributes assigned to water-level measurements from a well in Pahrump Valley.....	125
C-11—C-13.	Maps showing:	
C-11.	Spatial distribution and altitude of head observations in wells representing regional, steady-state conditions used in calibration of the Death Valley regional ground-water flow system model	126
C-12.	Spatial distribution and maximum drawdown of head observations in wells representing regional, transient conditions used in calibration of the Death Valley regional ground-water flow system model.....	127
C-13.	Spatial distribution and bottom depth of opening in head-observation wells (steady-state and transient conditions) used in calibration of the Death Valley regional ground-water flow system model	129
C-14.	Graphs showing uncertainty of 700 head observations computed to represent prepumped, steady-state conditions in the Death Valley regional ground-water flow system model domain. <i>A</i> , Cumulative frequency. <i>B</i> , Source of error.....	131

Tables

C-1.	Estimates of mean annual ground-water discharge from major evapotranspiration-dominated discharge areas in Death Valley regional ground-water flow system model domain.....	107
C-2.	Estimates of mean annual natural ground-water discharge from major spring areas not included in evapotranspiration-based discharge estimates in the Death Valley regional ground-water flow system model domain	109
C-3.	Number of wells and estimated total pumpage for 1913–98 by hydrographic area for the Death Valley regional ground-water flow system model domain	112
C-4.	Estimates of flow across lateral boundary segments of the Death Valley regional ground-water flow system model domain for prepumped conditions.....	120
C-5.	Annual volumetric flow estimates of major water-budget components of Death Valley regional ground-water flow system model domain for prepumped conditions and 1998 conditions	121
C-6.	Horizontal hydraulic-conductivity estimates of hydrogeologic units in the Death Valley regional ground-water flow system	122
C-7.	Description of attributes assigned to water levels retrieved from Ground-Water Site Inventory (GWSI) for simulation of ground-water flow in the Death Valley regional ground-water flow system model domain.....	124
C-8.	Bottom depth of open interval for wells used to calibrate the Death Valley regional ground-water flow system model.....	128

CHAPTER C. Hydrologic Components for Model Development

By Carma A. San Juan, Wayne R. Belcher, Randell J. Laczniak, and Heather M. Putnam

Introduction

Hydrologic components of the Death Valley regional ground-water flow system (DVRFS) were evaluated to support development of a ground-water flow model. The components evaluated are those affecting the water budget: the distribution and volume of natural ground-water discharge, ground-water pumpage, ground-water recharge, and lateral inflow and outflow; the hydraulic conductivity values of the major hydrogeologic units (HGUs); and water levels (fig. C-1). This information is used in Chapter D to conceptualize ground-water flow through the Death Valley region and in Chapter F to develop discharge and hydraulic-head observations for model calibration.

Although previous investigators have attempted to quantify all or some of these major flow components in parts of the DVRFS region (Malmberg and Eakin, 1962; Walker and Eakin, 1963; Hunt and others, 1966; Malmberg, 1967; Glancy, 1968; Rush, 1968; Miller, 1977; Waddell, 1982; Rice, 1984; Harrill, 1986; Harrill and others, 1988; Dettinger, 1989), only a few have developed comprehensive estimates for the entire DVRFS region (IT Corporation, 1996a and b; D'Agnesse and others, 1997). Attempts to combine results from past investigations often are complicated by uncertainties and differences in the definition of basin and study area boundaries (D'Agnesse and others, 2002).

A series of studies was conducted to reassess previous estimates of the major flow components and hydraulic properties of the DVRFS region to improve the data for the conceptual model and for model calibration as part of the DVRFS investigation. These studies, the results of which are described in this chapter, focused on refining estimates of natural ground-water discharge by developing local estimates of evapotranspiration (ET), and compiling and making additional spring-flow measurements; compiling ground-water pumpage information to estimate the history of ground-water development; estimating ground-water recharge from numerical simulations of net infiltration; estimating boundary inflow and outflow by using regional hydraulic gradients and water budgets of areas adjacent to the DVRFS model domain; estimating hydraulic properties from available literature and aquifer-test data; and evaluating available water-level data to estimate representative pre- and post-pumping hydraulic head

information. In general, existing and newly acquired data were evaluated using current technology and concepts, analyses were refined or new algorithms were implemented for making interpretations, and values appropriate for the regional extent and scale of the model were estimated.

Water Budget

A water budget is developed to evaluate the balance between the flow into and flow out of a ground-water flow system. The primary components of the water budget are natural discharge, recharge, and lateral flow into and out of an area across its boundary. The introduction of pumping as a discharge from the flow system initially decreases hydraulic heads and ultimately affects one or more flow components either by decreasing natural discharge or increasing recharge. The following sections describe these major flow components and provide estimates of each component as used in the development of the transient flow model of the DVRFS. Ground-water discharge estimates derived from estimates of ET computed from micrometeorological measurements and from spring-flow measurements are the primary mass-balance observations used to calibrate the transient flow model. Estimates of recharge and boundary flow, although quantified and discussed in this chapter, are based on model simulations or on less direct measurements. Together, these flow components also were used to develop a general water budget for pre-pumped and pumped conditions.

Ground-Water Discharge

Ground-water discharge from the DVRFS model domain occurs both naturally and nonnaturally. Natural ground water recharge occurs as ET and spring flow and, to a small extent, as lateral flow to adjacent basins. Nonnaturally, ground water discharges as artesian flow from wells (1913–45) or as pumpage from wells in agricultural areas such as Pahrump and Penoyer Valleys and the Amargosa Desert. Moreo and others (2003) estimated that by 1998 pumpage was equivalent to nearly 75 percent of the natural discharge estimated for the DVRFS model domain prior to ground-water development.

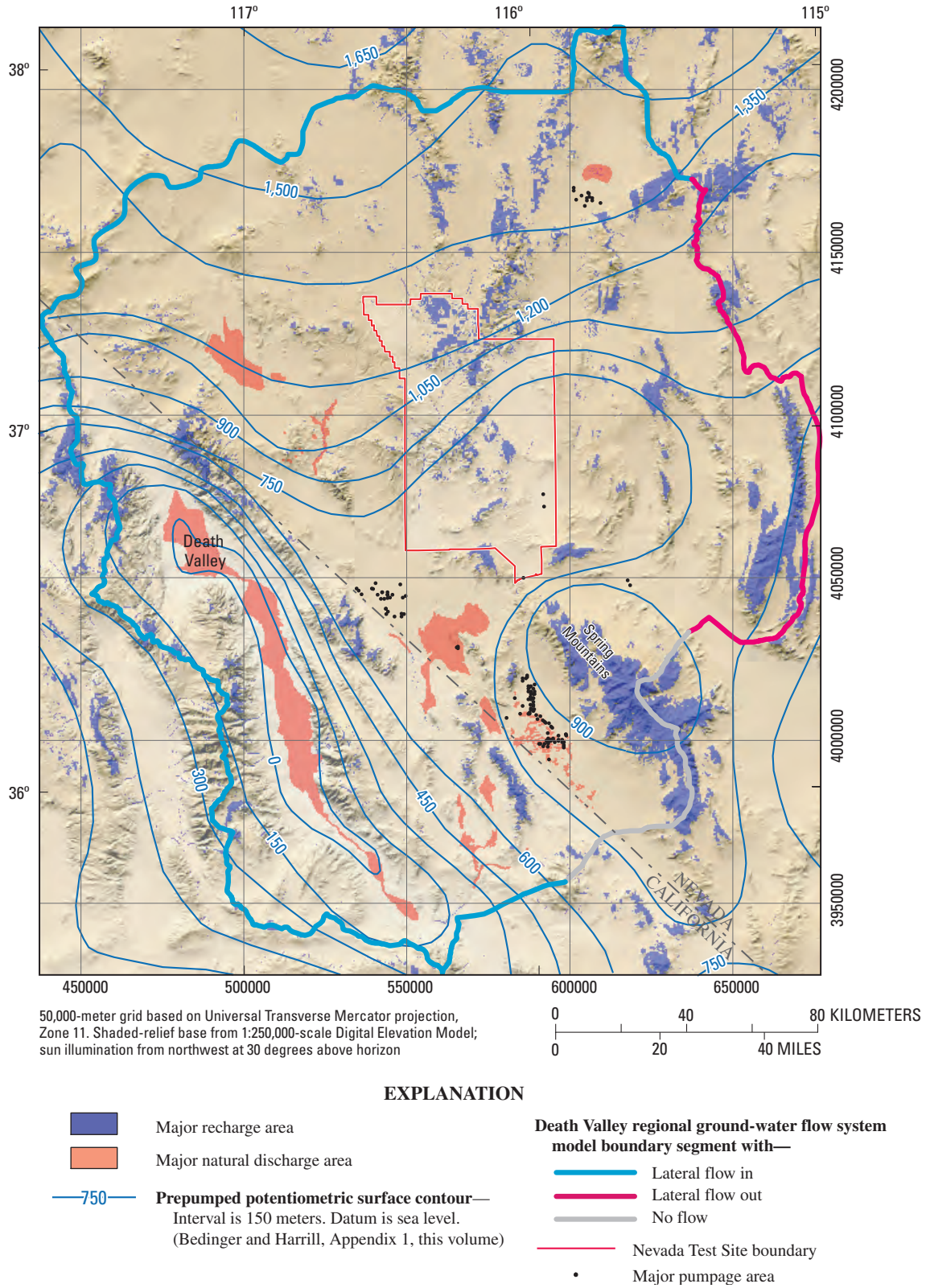


Figure C-1. Major areas of ground-water recharge, natural discharge, and pumpage, and model boundary segments of lateral flow in the Death Valley regional ground-water flow system region.

The following sections describe estimates of natural discharge and pumping as developed for simulating ground-water flow in the DVRFS model domain.

Natural Ground-Water Discharge

Areas of natural discharge cover less than 5 percent of the DVRFS model domain (fig. C-2). These areas include wet playas, wetlands with free-standing water or surface flow, narrow drainages lined with riparian vegetation, and broad areas of phreatophytic shrubs and grasses. The largest discharge areas by flow volume are Death Valley, Ash Meadows, and Sarcobatus Flat, respectively (fig. C-2). Each of these discharge areas represents a unique environment and together they include most of the different types of local habitat supported by ground-water discharge throughout the DVRFS region. Death Valley is dominated by a saltpan surrounded by alluvial fans and by numerous locally and regionally fed springs fringed with a variety of desert shrubs, trees, and grasses. Ash Meadows is a unique desert oasis that consists of broad wetlands fed by orifice-type springs. These large-volume springs are surrounded by extensive grass meadows interspersed with moderately dense to sparse stands of trees and shrubs. Sarcobatus Flat is a broad playa surrounded by moderately dense grasses and sparse shrubs that are supported by a few small springs and seeps and a moderately shallow water table.

The quantity of ground water discharging from most of the major discharge areas in the DVRFS model domain (fig. C-2) has been estimated in previous studies. These estimates were developed primarily from spring-flow measurements, ET estimates, or a combination of both. Usually, ground-water discharge was estimated only for an individual discharge area or at a specific location, and not for the entire flow system. Reports estimating ground-water discharge are Malmberg and Eakin (1962), Walker and Eakin (1963), Pistrang and Kunkel (1964), Hunt and others (1966), Malmberg (1967), Glancy (1968), Rush (1968), Van Denburgh and Rush (1974), Winograd and Thordarson (1975), Miller (1977), Harrill (1986), Czarnecki (1997), D'Agnese and others (1997), Laczniaik and others (1999), Reiner and others (2002), and DeMeo and others (2003). Discrepancies in discharge estimates between more recent and previous reports typically reflect differences in the delineation of the area contributing to ET, the number of springs measured, ET rates estimated for vegetation types, or some combination thereof (Laczniaik and others, 2001, p. 31; D'Agnese and others, 2002, p. 26).

Evapotranspiration

Recent investigations of natural ground-water discharge in the DVRFS region estimate discharge by calculating ET. The underlying assumption of this approach is that most of the ground water issuing from springs and seeps within the discharge area ultimately is evaporated or transpired locally in the DVRFS region and therefore is accounted for in estimates of ET. Most of the discharge data used to develop the discharge observations presented in Chapter F (this volume) are based

on estimates of ET in recent reports by Laczniaik and others (1999 and 2001), Reiner and others (2002), and DeMeo and others (2003). The report by Laczniaik and others (2001) is the most comprehensive evaluation of ground-water discharge in that it provides estimates of ground-water discharge for 9 of the 15 major ET-dominated discharge areas in the DVRFS model domain (fig. C-2). Their estimate of discharge in Oasis Valley was revised in a subsequent study (Reiner and others, 2002). Laczniaik and others (2001) made no attempt to revise estimates of natural discharge from Pahrump and Penoyer Valleys because ground water withdrawn for irrigation had locally altered the distribution of native vegetation and decreased local spring flow. D'Agnese and others (2002, p. 26) provide an estimate of natural discharge from Pahrump Valley but state that their estimate was based on an ET analysis that used a map delineating the native phreatophyte distribution in 1959-61 (Malmberg, 1967, pl. 3)—a time by which vegetation already had been significantly affected by local pumping. These same authors present an estimate of natural discharge from Penoyer Valley that was first documented in a reconnaissance report by Van Denburgh and Rush (1974, p. 23) and later reported by IT Corporation (1996a). A recent study by DeMeo and others (2003) was the primary source used to develop estimates of ground-water discharge from the floor of Death Valley.

The more recent investigations were similar in that continuous micrometeorological data were collected to estimate local ET rates, and remotely sensed multi-spectral data were used to distribute measured ET rates over the area evaluated. Micrometeorological data were collected continuously at 15 stations for 1 to 3 years each in Ash Meadows and Oasis Valley (Laczniaik and others, 1999; Reiner and others, 2002) and at 6 sites in Death Valley over a 4-year period (DeMeo and others, 2003). Remotely sensed images, aerial photographs, and soils and wetland maps were integrated using geographic information system (GIS) techniques and were used in these studies to delineate ET units (areas of similar vegetation and moisture conditions) and distribute calculated ET rates over respective discharge areas. This process resulted in more consistent and generally improved estimates of ground-water discharge than in previous studies.

Most ET-based estimates of ground-water discharge assume that in addition to ground water, all precipitation falling on a discharge area, any surface water flowing into a discharge area, and all local infiltration to the shallow flow system ultimately are evaporated or transpired by the local vegetation. Accordingly, mean annual ground-water discharge (estimated from ET) is the difference between the mean annual ET and the sum of mean annual precipitation and any surface-water inflow. In more recent studies, mean annual ET is computed by multiplying the area of an ET unit by the mean annual ET rate calculated for a unit. Mean annual ET rates for individual ET units range from less than 0.06 meter (m) for bare and salt-encrusted soil (DeMeo and others, 2003) to 2.75 m for open water (Laczniaik and others, 2001). Adjustments made for precipitation were typically small because mean annual precipitation ranges from less than 0.08 m in

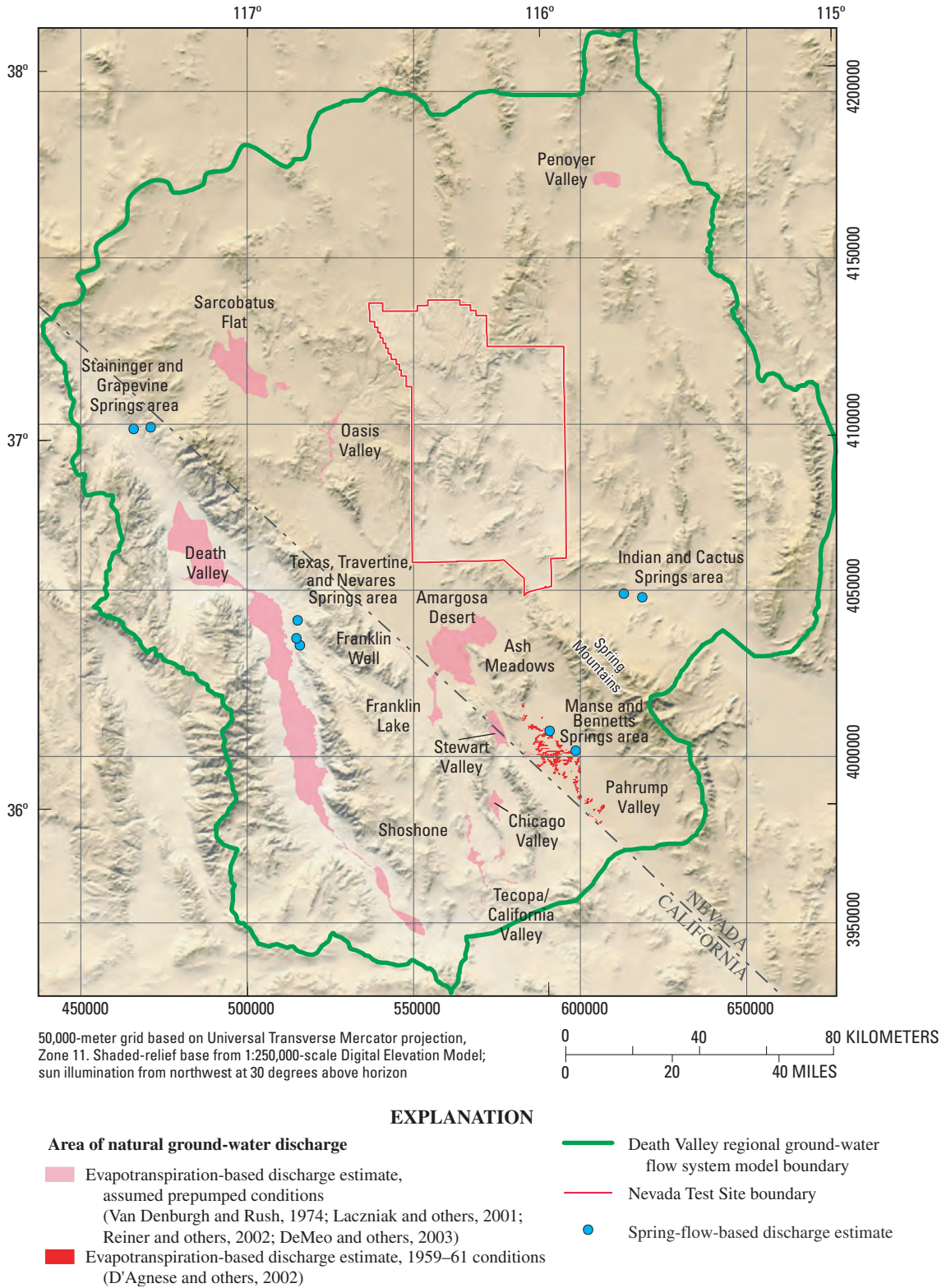


Figure C-2. Major areas of natural ground-water discharge in the Death Valley regional ground-water flow system model domain.

Death Valley (DeMeo and others, 2003) to about 0.15 m in Sarcobatus Flat and Oasis Valley (Laczniaik and others, 2001). Runoff into major discharge areas from adjacent highlands was assumed to be minimal and was not calculated. Accordingly, ground-water discharge for most major ET-dominated discharge areas (fig. C-2) was calculated as the difference between mean annual ET and mean annual precipitation.

Accurate mapping of soil and vegetation in discharge areas was critical to improving estimates of the size of ET units. These more recent studies identified most of the vegetation, soil, and water-dominated ET units in major discharge areas using remotely sensed, spectral imagery acquired during 1989–96. Wetland maps produced by the U.S. Fish and Wildlife Service for the National Wetlands Inventory Project were used to delineate two soil-dominated ET units—bare and salt encrusted—in Death Valley (DeMeo and others, 2003). Other ET units included areas of open playa; sparse to dense vegetation; moist, bare soil; and open water (Laczniaik and others, 2001; Reiner and others, 2002). Death Valley, the largest discharge area, has an estimated area of about 445.5 square kilometers (km²) and is dominated by extensive flats of moist, bare, and salt-encrusted soil. Sarcobatus Flat has an estimated area of about 138.6 km² and is predominantly sparse to moderately dense shrubland. The fourth largest ET area, Ash Meadows, has an area of about 50.5 km² and ranges from

broad, sparse grassland to dense, riparian wetland adjacent to spring pools. The estimated sizes of the other major ET-dominated major discharge areas are given in table C-1.

Micrometeorological data were collected continuously and averaged over 20-minute periods. These 20-minute averages were used to compute ET rates for the different ET units delineated throughout the DVRFS region. Microclimate stations were operated at 10 sites in Ash Meadows from 1993 to 1997 (Laczniaik and others, 1999, table 6), at 5 sites in Oasis Valley from 1996 to 2000 (Reiner and others, 2002, table 3), and at 6 sites in Death Valley from 1997 to 2001 (DeMeo and others, 2003, table 3). Annual ET rates were computed from the micrometeorological data using the Bowen ratio solution of the energy-budget equation (Bowen, 1926). Average annual ET rates for ET-dominated discharge areas ranged from 0.20 meter per year (m/yr) in Stewart Valley to 0.79 m/yr in Pahrump Valley (table C-1).

Mean annual ground-water discharge for each major ET-dominated discharge area was calculated as the product of the adjusted-annual ET rate and the area of the ET unit (table C-1). Annual ET rates were adjusted by removing water contributed by local precipitation. Although a comparison of these and previous discharge estimates is complicated by differences in the procedures used to estimate ET rates and in the mapped extent of individual discharge

Table C-1. Estimates of mean annual ground-water discharge from major evapotranspiration-dominated discharge areas in Death Valley regional ground-water flow system model domain.

[Ground-water discharge rounded to nearest thousand. Rates rounded to nearest hundredth. Mean annual ground-water discharge may not equal product of precipitation-adjusted ET rate and area because of rounding. Dash (--) indicates that no value was reported in referenced source or that the information given was insufficient to compute a value. Abbreviations: ET, evapotranspiration; m/yr, meters per year; km², square kilometer; m³, cubic meter; Mm³, million cubic meters]

Discharge area (shown in fig. C-2)	Estimated mean annual ET rate (m/yr)	Area (km ²)	Annual precipitation rate (m/yr)	Estimated precipitation- adjusted annual ET rate (m/yr)	Estimated mean annual ground-water discharge (m ³)
Ash Meadows ¹	0.55	50.5	0.11	0.44	22,203,000
Chicago Valley ¹	0.34	2.48	0.11	0.23	530,000
Franklin Lake ¹	0.23	9.43	0.10	0.13	1,234,000
Franklin Well area ¹	0.46	1.20	0.11	0.35	432,000
Oasis Valley ²	0.70	13.9	0.15	0.55	7,401,000
Pahrump Valley ³	0.79	12.2	0.12	0.67	³ 8,082,000
Penoyer Valley ⁴	--	76.9	--	0.06	4,650,000
Sarcobatus Flat ¹	0.27	138.6	0.15	0.12	16,035,000
Shoshone area ¹	0.55	5.62	0.09	0.46	2,590,000
Stewart Valley ¹	0.20	12.2	0.11	0.09	1,234,000
Tecopa/California Valley area ¹	0.64	14.2	0.09	0.55	7,894,000
Death Valley floor ⁵	--	445.5	--	0.01	⁶ 43,172,000
Total					115,457,000

¹Laczniaik and others (2001, tables 5 and 10).

²Reiner and others (2002, table 5).

³D'Agnesse and others (2002, table 3). Mean annual ground-water discharge during the period 1959–61.

⁴Van Denburgh and Rush (1974, table 8 and p. 23); D'Agnesse and others (2002, p. 26).

⁵DeMeo and others (2003, table 4).

⁶Estimate varies from about 27.1–43.2 Mm³ as adjusted for different flood recurrence intervals (DeMeo and others, 2003, p. 24). Flood-adjusted ET estimate reported by DeMeo and others (2003, p. 24) is 40.7 Mm³.

areas, Laczniaik and others (2001, p. 29–30) state that their estimates, in general, are greater than those reported in the literature for the more northern discharge areas and less than those previously reported for the more southern discharge areas.

The mean annual ground-water discharge given for Death Valley (DeMeo and others, 2003, p. 24) is considered a partial estimate because evaporation, transpiration, and flow diversions associated with a series of regional springs along the northeastern margin of the valley are not included. The total mean annual ground-water discharge from Death Valley is equal to the sum of ET estimated for the valley floor and reported flow from valley-margin springs discussed in the following section. This method may account twice for underflow from these valley-margin springs into sediment beneath the valley floor. The error resulting from any double accounting of underflow is expected to be small because most of the water discharged from these springs is transpired, evaporated, or diverted for local water supply.

All discharge estimates given in table C–1, except those for Pahrump and Penoyer Valleys, are assumed to represent discharge for both prepumped and current conditions. This assumption is reasonable considering that pumping from these major discharge areas is negligible and climate has been relatively stable over the period. The total amount of ground water discharging annually from the DVRFS model domain (computed by summing all estimates in table C–1) is about 115.5 million cubic meters (Mm³).

Limitations inherent in an ET-based approach for estimating ground-water discharge can be attributed to errors in delineating the extent of ET units and errors in calculating ET rates (Laczniaik and others, 2001, p. 31). Other factors potentially affecting the accuracy of ET-based estimates of ground-water discharge include (1) the assumption that all spring flow ultimately is evaporated or transpired from within the discharge area, (2) the assumption that surface-water inflow is minimal, (3) the short period of record used to compute mean annual ET rates, (4) the limited number of local sites used to estimate mean annual ET rates, (5) uncertainties associated with estimating ET on the basis of relative differences in vegetation density, and (6) uncertainties in the amount of water contributed by precipitation and surface flow to the ET estimates (Laczniaik and others, 2001, p. 31).

Springs

Most of the ground water discharged naturally from the DVRFS region flows from springs and seeps. Regional high-volume springs having flows greater than 1,500 cubic meters per day (m³/d) discharge in Oasis Valley, Ash Meadows, Pahrump Valley, the Shoshone and Tecopa areas, and on the floor of Death Valley (fig. C–2). Typically, these regional springs discharge water with temperatures greater than 30 degrees Celsius (°C) (U.S. Geological Survey, National Water Information System, retrieved June 2003) directly from the rocks that make up the regional aquifer. Because most flow from

springs and seeps in major ET-dominated discharge areas is evaporated and(or) transpired by the local riparian vegetation, ET estimates are assumed to be inclusive of spring and seep flow (table C–1; Laczniaik and others, 2001; Reiner and others, 2002).

Spring discharge cannot always be quantified accurately using ET-based methods. For example, ET-based methods are not well suited for estimating discharge in areas where springs support limited vegetation or where local pumping has decreased spring flow. Estimates of ground-water discharge from areas of spring flow not estimated by an ET technique were derived solely on the basis of spring-flow measurements and are presented in table C–2. Areas of discharge not included in ET-based estimates are the Staininger and Grapevine Springs areas near Scotty's Castle in Death Valley; Texas, Travertine, and Nevares Springs areas near Furnace Creek Ranch in Death Valley; Indian and Cactus Springs areas near Indian Springs, Clark County, Nev.; and the Manse and Bennetts Springs areas in Pahrump Valley (fig. C–2). All discharge estimates, except those for Pahrump Valley (Bennetts and Manse Springs), were based on flow measurements made or compiled by C.S. Savard (U.S. Geological Survey, written commun., 2001). Thus any nonreferenced discharge values in the following sections are attributed to Savard's unpublished work. The total annual discharge from spring flow summarized in table C–2 is about 16.8 Mm³.

Staininger and Grapevine Springs

Mean ground-water discharge from Staininger Spring, the water supply for Scotty's Castle area in Death Valley, is estimated at 1,035 m³/d±15 percent (table C–2). This estimate was based on four historical flow measurements, three of which were reported by Miller (1977): 1,019 m³/d in 1924, 981 m³/d in 1958, 1,025 m³/d in 1971, and the fourth, 1,090 m³/d in 1967 by Rush (1968). Other reported values of discharge from this spring—2,271 m³/d (Ball, 1907), 54 m³/d (Waring, 1915), and 163 m³/d (Waring, 1965)—were considered to be unreliable because they did not measure the entire spring flow.

The aggregate discharge from about 12 springs and seeps in the Grapevine Springs area is estimated at 2,450 m³/d±20 percent (table C–2). This estimate was originally made by Miller (1977) on the basis of discharge measurements made at a few accessible springs and a cursory quantification of ET. Previous reports by Ball (1907) and Mendenhall (1909) mention these springs but do not provide a discharge estimate. Rush (1968) reports discharge from a single unnamed spring at 109 m³/d.

Texas, Travertine, and Nevares Springs

Discharge from Texas Spring from 1989 to 1996 is estimated at 1,220 m³/d±15 percent (table C–2). This estimate is based on measurements reported in LaCamera and Westenburg (1994), Hale and Westenburg (1995), Westenburg and LaCamera (1996), LaCamera and others (1996), and

Table C-2. Estimates of mean annual natural ground-water discharge from major spring areas not included in evapotranspiration-based discharge estimates (table C-1) in the Death Valley regional ground-water flow system model domain.

[--, no value reported; m³/d, cubic meters per day; discharge rate rounded to nearest five; ground-water discharge rounded to nearest hundred]

Spring name/area	General location	Estimated mean discharge rate (m ³ /d)	Estimated mean annual ground-water discharge (m ³)	Estimated percent accuracy
Staininger Spring ¹	Scotty's Castle, Death Valley, Calif.	1,035	378,000	15
Grapevine Springs ¹	Scotty's Castle, Death Valley, Calif.	2,450	894,900	20
Texas Spring ¹	Furnace Creek Ranch, Death Valley, Calif.	1,220	445,600	15
Travertine Spring ¹	Furnace Creek Ranch, Death Valley, Calif.	4,630	1,691,100	10
Nebares Spring ¹	Furnace Creek Ranch, Death Valley, Calif.	1,885	688,500	--
Indian and Cactus Springs ¹	Indian Springs, Clark County, Nev.	2,240	818,200	10
Bennetts and Manse Springs ²	Pahrump, Nev.	32,400	11,834,100	25
Total		45,860	16,750,400	--

¹Estimate based on flow measurements made or compiled by C.S. Savard (U.S. Geological Survey, written commun., 2001).

²Estimate of ground-water discharge based on flow measurements from Bennetts and Manse Springs made before 1913 when ground-water pumping began (Maxey and Jameson, 1948; Malmberg, 1967; and Harrill, 1986).

LaCamera and Locke (1997). Earlier reports give discharge rates from Texas Spring that range from 136 m³/d in 1915 (Waring, 1915) to 685 m³/d in 1926 (Pistrang and Kunkel, 1964). A tunnel constructed into the spring between 1926 and 1941 nearly doubled spring discharge. Reported discharge measurements taken after tunnel construction were 930 m³/d in 1941 (Pistrang and Kunkel, 1964); 1,150 to 1,223 m³/d from 1956 to 1963 (Pistrang and Kunkel, 1964); and 1,145 m³/d in 1976 (Miller, 1977).

Mean discharge from the Travertine Spring area is estimated at 4,630 m³/d±10 percent. This estimate is based on measurements made from 1956 to 1972 (table C-2; Miller, 1977). Estimates developed by summing measurements made at 10 springs in the Travertine Springs area between 1955 and 1965 ranged from 4,111 to 4,747 m³/d (Pistrang and Kunkel, 1964). The aggregate discharge estimate of 3,815 m³/d given in Miller (1977) was based on measurements made at only three springs in 1977. Other periodic measurements made at individual springs are difficult to composite into an estimate of discharge for the entire area because of differences in measurement dates.

Natural discharge from the Nebares Spring area is estimated at 1,885 m³/d (table C-2; Pistrang and Kunkel, 1964). This estimate includes discharge from nearby Cow (100 m³/d) and Salt Springs (25 m³/d). Early measurements of discharge from the main area of Nebares Spring averaged 1,470 m³/d for the period 1956 to 1957, while discharge from other nearby springs in the Nebares Spring area totaled 290 m³/d (Pistrang and Kunkel, 1964). Hunt and others (1966) report combined discharge from the five major springs in the area at 1,790 m³/d in 1951 and 1,760 m³/d in 1957. An aggregate discharge of about 1,420 m³/d was reported by Miller (1977) for Nebares Spring and a nearby, unnamed spring.

Indian and Cactus Springs

Discharge from the Indian and Cactus Springs area is estimated at 2,240 m³/d±10 percent (table C-2). The first reported estimate of discharge at Indian Springs, 2,230 m³/d (Carpenter, 1915), was made in 1912. Subsequent estimates of 2,180 m³/d (Maxey and Jameson, 1948) and 2,365 m³/d (Malmberg, 1965) varied by less than 10 percent. Rush (1970) reports an anomalously low discharge of 1,690 m³/d. He attributes the decrease to be an effect of nearby pumping. Reported estimates of discharge from Cactus Spring are all less than 5 m³/d (Carpenter, 1915; Maxey and Jameson, 1948).

Bennetts and Manse Springs

Natural discharge from Bennetts and Manse Springs in Pahrump Valley (fig. C-2) is estimated at 32,400 m³/d±25 percent (table C-2) for the period prior to ground-water pumping. This estimate is based on reported discharges before 1913 of 17,900 m³/d from Bennetts Spring and 14,500 m³/d from Manse Spring (Maxey and Jameson, 1948). The estimates of spring flow from Bennetts and Manse Springs are based on measurements made before 1913 and represent prepumped conditions (Maxey and Jameson, 1948; Malmberg, 1967; and Harrill, 1986). The relatively large inaccuracy given to the estimate accounts for uncertainties associated with the nature of the measurements.

Bennetts and Manse Springs were the largest springs in Pahrump Valley and discharged from the base of alluvial fans at the foot of the Spring Mountains. After 1945, large-scale agricultural development accompanied by the drilling and pumping of wells to irrigate cropland drastically decreased spring flows throughout the valley (Harrill, 1986). Bennetts Spring stopped flowing in 1959. Manse Spring virtually

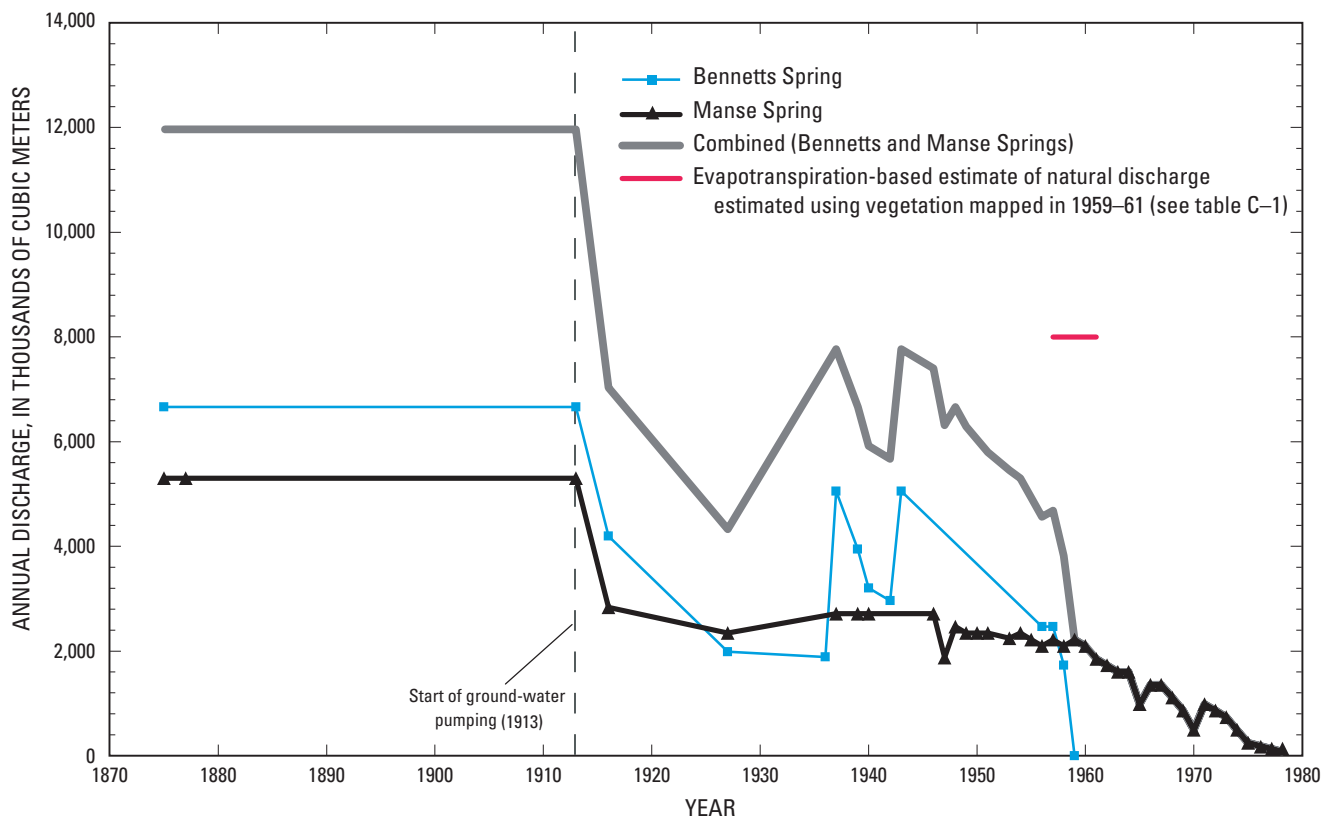


Figure C-3. Annual discharge from regional springs in Pahrump Valley, Bennetts and Manse Springs, 1875–1978.

stopped flowing in 1977 although small intermittent flows during the winter season have been reported. Estimated annual discharge from Bennetts and Manse Springs is shown in figure C-3 for 1875–1978.

The mean annual discharge in Pahrump Valley estimated from ET by D’Agnese and others (2002) also is shown in figure C-3. During 1959–61, mean annual discharge was estimated as about 8.1 Mm³.

Pumpage

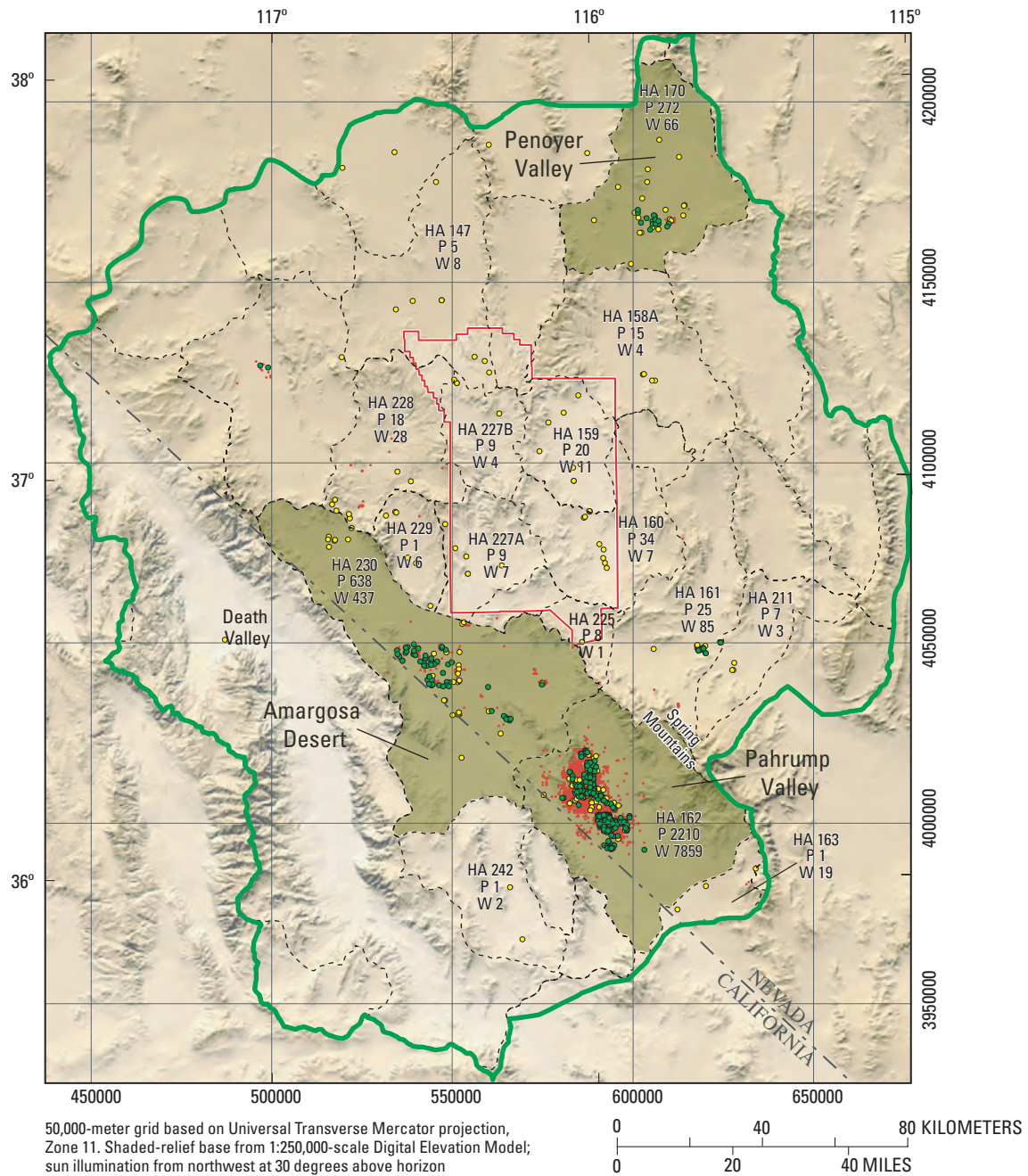
Substantial quantities of ground water have been pumped from the DVRFS region. Ground-water pumping started around 1913 in Pahrump Valley to support a small agricultural community and has continued throughout the region to support local agriculture, mining, industry, and rural and urban growth. The number of pumping wells in the DVRFS region increased substantially from only a few wells in 1913 to nearly 9,300 wells in 1998 (Moreo and others, 2003).

Pumpage from wells, and the physical description and location of pumping wells in the DVRFS region, are reported intermittently in publicly available reports and databases. These sources lack sufficient information, however, from which to develop the complete history of ground-water development for the DVRFS region. Moreo and others (2003) compiled available information and developed annual pumpage

estimates to complete the annual pumpage history for the period 1913–98. Their database contains estimates of annual ground-water withdrawal at each known pumping well in the DVRFS region and was used to develop pumping stresses for model simulation of pumped conditions (see Chapter F, this volume).

About 8,600 of the approximately 9,300 wells investigated by Moreo and others (2003) are in the DVRFS model domain (fig. C-4). A few wells included in Moreo and others (2003) that had estimated open intervals that did not match the interpolated horizons in the hydrogeologic framework model (Chapter E, this volume) were removed from the dataset. The combined pumpage from these few wells removed from the data set accounted for less than 0.001 percent (about 8,000 m³ of the total ground water pumped for the period 1913–98).

About 97 percent of the pumping wells are in the southern part of the model domain (fig. C-4 and table C-3). These wells are concentrated primarily in the southern part of Amargosa Desert and in Pahrump Valley. Penoyer Valley has the greatest concentration of pumping wells in the northern part of the model domain. About 95 percent of the pumpage estimated from 1913 to 1998 was withdrawn from these three hydrographic areas (fig. C-4 and table C-3) delineated by Cardinali and others (1968) on the basis of topographic basins. Table C-3 presents estimates of total pumpage from the DVRFS model domain for the period 1913–98 and for



EXPLANATION

- Hydrographic areas where pumpage exceeds 100 million cubic meters (Mm^3)
- HA 242
P 1
W 2 Hydrographic areas where pumpage exceeds 1 Mm^3 —
HA, hydrographic area;
P, total pumpage in Mm^3 ;
W, number of wells.
- Hydrographic area boundary
(modified from Cardinalli and others, 1968)
- Death Valley regional ground-water flow system model boundary
- Nevada Test Site boundary
- Pumping wells by water-use class**
(Moreo and others, 2003)
- Domestic
- Mining, public supply, and commercial
- Irrigation

Figure C-4. Spatial distribution of pumping wells by water-use class and total pumpage for 1913–98 by hydrographic area.

Table C-3. Number of wells and estimated total pumpage for 1913–98 by hydrographic area for the Death Valley regional ground-water flow system model domain.

[Annual pumpage estimates computed from data in Moreo and others (2003) for 22 hydrographic areas having reported pumpage; m³, cubic meters; pumpage values for 1913–98 are rounded to the nearest thousand and for 1998 to the nearest ten]

Hydrographic area		Number of wells 1913–98	Estimated pumpage	
Number	Name		1913–98 (m ³)	1998 (m ³)
144	Lida Valley	1	12,000	860
146	Sarcobatus Flat	15	850,000	25,160
147	Gold Flat	8	4,561,000	43,170
148	Cactus Flat	2	866,000	56,740
158A	Emigrant Valley	4	15,196,000	345,380
159	Yucca Flat	11	20,023,000	91,280
160	Frenchman Flat	7	34,272,000	534,100
161	Indian Springs Valley	85	25,422,000	789,680
162	Pahrump Valley	7,859	2,210,135,000	43,855,360
163	Mesquite Valley ¹	19	1,059,000	31,080
170	Penoyer Valley	66	272,390,000	15,669,790
173A	Railroad Valley ¹	2	197,000	4,930
211	Three Lakes Valley (southern part)	3	6,986,000	410,750
225	Mercury Valley	1	8,479,000	3,700
226	Rock Valley	1	38,000	860
227A	Fortymile Canyon (Jackass Flats)	7	8,510,000	184,650
227B	Fortymile Canyon (Buckboard Mesa)	4	8,674,000	117,180
228	Oasis Valley	28	17,880,000	309,600
229	Crater Flat	6	1,094,000	171,450
230	Amargosa Desert	437	637,619,000	30,729,610
242	Lower Amargosa Desert	2	1,132,000	33,300
243	Death Valley	1	497,000	40,700
Total		8,569	3,275,892,000	93,449,330

¹Only part of hydrographic area contained in Death Valley regional ground-water flow system model domain.

1998 by hydrographic area. Of the 38 hydrographic areas in the DVRFS model domain, 16 have no reported pumping during this period.

Moreo and others (2003) grouped pumping wells into three water-use categories: (1) irrigation; (2) mining, public supply, and commercial; and (3) domestic. Although nearly 93 percent of the wells are for domestic use, 90 percent of the water pumped was for irrigation. Pumpage determined for each water-use category was estimated using different methods. The results and techniques used to develop a pumpage history for the DVRFS region are summarized in the following paragraphs. Moreo and others (2003) provide more detail.

Well-construction information was used to estimate the open-interval depths of each pumping well. Approximately 85 percent of the irrigation wells, 97 percent of the mining, public supply, and commercial wells, and 98 percent of the domestic wells had reported completion intervals (Moreo and others, 2003). For wells for which construction information was absent, open intervals were estimated using construction data from nearby wells of the same water-use category. Moreo

and others (2003) reported that most pumping wells are open to basin-fill deposits and were drilled to depths of less than about 150 m, with less than 1 percent having depths exceeding about 300 m.

Irrigation accounted for 90 percent of the ground water pumped from the DVRFS model domain during 1913–98. Irrigation gradually declined from about 100 percent (about 4,940 Mm³) of the ground water used in 1913 to about 80 percent (about 74,710 of 93,450 Mm³) in 1998 (fig. C-5). Moreo and others (2003) estimated annual irrigation by multiplying an irrigated acreage by a crop application rate. These investigators identified the extent and years that a field was irrigated from pumping inventories and remotely sensed data available since 1972; the crop type from pumping inventories and field visits; and the application rate of the representative crop from published sources. Application-rate estimates for alfalfa had the greatest effect on estimated pumpage. The high sensitivity of application rates, particularly that of alfalfa, is not unexpected considering that 75 percent of the ground water withdrawn from 1913–98 was used to irrigate alfalfa (Moreo

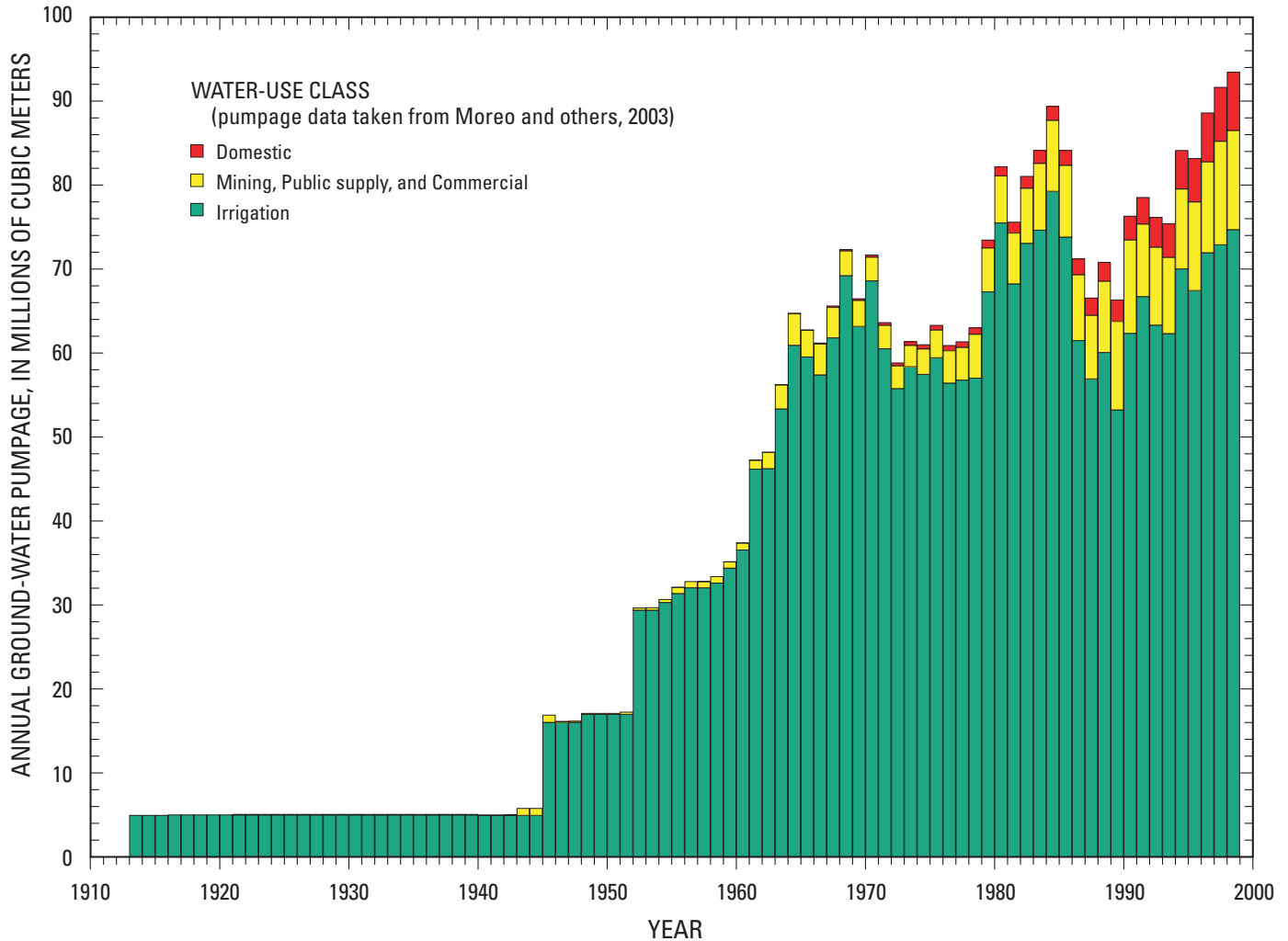


Figure C-5. Annual ground-water pumpage estimates developed by water-use class from Death Valley regional ground-water flow system model domain, 1913–98.

and others, 2003). The uncertainty in annual irrigation was expressed by Moreo and others (2003) as a range between a minimum and maximum estimate, with the most likely value closer to the minimum.

Mining, public supply, and commercial pumpage accounted for about 8 percent of all the ground water pumped from 1913–98. By 1998 pumpage in this category increased, accounting for nearly 13 percent of the annual total (fig. C-5). Pumpage for mining, public supply, and commercial use was estimated primarily from metered and inventoried data. Estimates for this water-use category were considered accurate within 5 percent (Moreo and others, 2003).

Pumpage for domestic use accounted for about 2 percent of the total amount of ground water pumped from 1913 to 1998. The percentage of water pumped for domestic use gradually increased over the years and by 1998 accounted for more than 7 percent of the annual total (fig. C-5). Moreo and others (2003) estimated domestic pumpage as the product of the average annual rate (per household) of domestic consumption and

the number of domestic wells permitted for use. The number of domestic wells may have been slightly overestimated because the history of well abandonment is not known. The uncertainty in the domestic-use estimate was expressed as a range defined by a minimum and maximum value that reflects, primarily, the uncertainty in the per household consumption rate. The minimum estimate of domestic pumpage was based on an annual per household consumption of 616.5 m³ and the maximum estimate on an annual per household consumption of 1,233 m³ (Moreo and others, 2003).

Annual ground-water pumpage estimates from the DVRFS model domain increased from about 5 Mm³ in 1913 to about 93.5 Mm³ in 1998 (fig. C-5 and table C-3). The greatest number of wells and the largest withdrawals are in Pahrump Valley, Amargosa Desert, and Penoyer Valley (fig. C-4). During 1913–45, ground water was used primarily for irrigation and was supplied by about 30 flowing wells in Pahrump Valley (Moreo and others, 2003). After 1945, local water use relied on pumps and continued to increase as access to the region

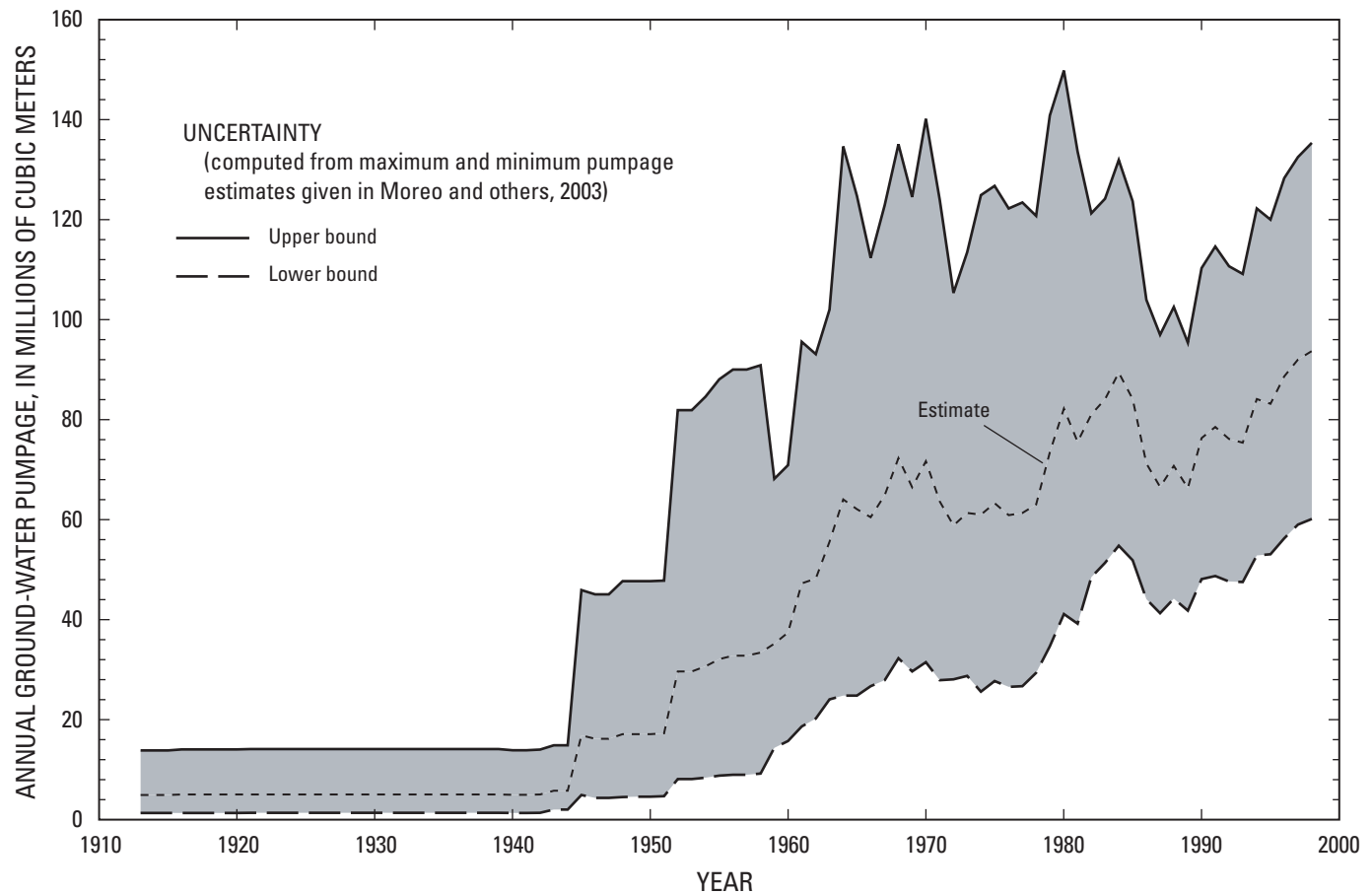


Figure C-6. Uncertainty in annual ground-water pumpage estimates developed for Death Valley regional ground-water flow system model domain, 1913–98.

improved (fig. C-5; Moreo and others, 2003). The percentage of ground water pumped for nonirrigation uses (domestic, mining, public supply, and commercial) began to increase from only a small percentage in 1960 to about 20 percent of the annual total in 1998. This trend is expected to continue as the population of Pahrump Valley and Amargosa Desert increases as a consequence of continued urbanization.

The total amount of ground water pumped from the DVRFS model domain during the period 1913–98 is estimated at 3,276 Mm³ (table C-3). Moreo and others (2003) expressed uncertainty in their estimate of annual pumpage as a range defined by a minimum and maximum estimate (fig. C-6). Accordingly, the uncertainty in their estimate of total pumpage from the DVRFS model domain during the period 1913–98 ranges from 1,616 to 6,081 Mm³. This large uncertainty is attributed to incomplete pumping records, misidentification of crop type, and errors associated with estimating annual domestic consumption, the irrigated area, and crop application rates (Moreo and others, 2003). The error associated with the uncertainty in the application rate, which differs spatially and temporally with variations in potential ET, length of growing season, irrigation systems, crop type, and management practices, exceeds that of all other uncertainties combined (Moreo and others, 2003).

Moreo and others (2003) did not adjust estimates of annual pumpage for water potentially returned to the flow system through subsequent infiltration of excess irrigation, lawn water, or septic tank wastewater. Although some return flow is likely to occur in the DVRFS model domain, the magnitude and timing of these returns have not been precisely quantified. Harrill (1986, p. 19) estimates return flows for Pahrump Valley as 70 percent of domestic pumpage, 50 percent of public-supply and commercial pumpage, and 25 percent of irrigation pumpage and states that the returns depend on the timing and method by which the water is returned to the flow system.

Stonstrom and others (2003) estimate return flows beneath three irrigated fields in the southern part of the Amargosa Desert. These estimates are made using the chloride mass-balance method and downward velocities inferred from peaks of chloride and nitrate concentrations noted in borehole depth profiles. Estimates of the rate at which irrigation water percolates downward through the unsaturated zone toward the water table ranged from 0.1 to 0.5 m/yr. On the basis of these rates and the depth to water beneath the fields, irrigation returns would take between 10 and 70 years to reach the water table. The water returned to the water table beneath individual irrigated fields was estimated to be 8 to 16 percent of the irrigation (Stonstrom and others, 2003, p. 19).

Many difficulties are associated with estimating return flows. These include uncertainties in pumpage, in the hydraulic properties of unsaturated zone sediment, and delineating the actual areas where water is or was returned to the environment. For example, ground water pumped for irrigation does not return to the flow system at the well (point of withdrawal) but rather to the water table beneath the field or fields irrigated by the well. The actual location of these fields, especially those of historical significance, can be highly uncertain. Despite these uncertainties, a method was developed to compute informal estimates of return flow. Return flows were computed as the product of the estimated annual pumpage and a user-defined return-flow percentage, and could be lagged in time by a user-defined value. All computed return flows were assumed to return to the water table at the location of the pumped well. Return flows were evaluated using the transient model in Chapter F of this volume.

Ground-Water Recharge

Ground-water recharge is defined as water that infiltrates downward through the unsaturated zone into the water table. Most of the ground-water recharge in the DVRFS region originates from precipitation that falls on mountainous areas throughout the DVRFS region (fig. C-7). The distribution and quantification of recharge for basins in the DVRFS region have been evaluated using empirical (Maxey and Eakin, 1950; Malmberg and Eakin, 1962; Walker and Eakin, 1963; Malmberg, 1967; Winograd and Thordarson, 1975; Miller, 1977; Harrill, 1986; IT Corporation, 1996a; D'Agnesse and others, 1997), water-balance (Rice, 1984; West, 1988), chloride mass-balance (Dettinger, 1989; Lichty and McKinley, 1995; Russell and Minor, 2002), and distributed-parameter (Hevesi and others, 2002; Hevesi and others, 2003) methods. Each of these methods attempts to capture the complex array of factors that control recharge.

The distributed-parameter method described by Hevesi and others (2003) provided an estimate of the potential recharge based on net infiltration, and was used primarily to distribute recharge in the model domain. The potential recharge estimated by their method was adjusted across the model domain to better balance with discharge (Chapter F, this volume). Hevesi and others (2003) estimated potential recharge using a net-infiltration model, INFILv3. Net infiltration is considered a reasonable indicator of ground-water recharge because most of the net infiltration and surface runoff that originates as precipitation in the model domain eventually moves downward through the unsaturated zone to recharge the ground-water flow system (Hevesi and others, 2003). In general, the uncertainty of approximating potential recharge from net infiltration increases as the thickness and heterogeneity of the unsaturated zone increases. INFILv3 simulates surface-water flow, snowmelt, transpiration, and ground-water drainage in the root zone and has as a climate algorithm that simulates daily climate conditions in local watersheds. Topography, geology, soils, and vegetation data are input to represent

local drainage-basin characteristics. Improved vegetation distributions were delineated from a western region vegetation map developed by the U.S. Geological Survey Gap Analysis Program (WESTVEG GAP) and soil distributions from the U.S. Department of Agriculture (1994) State Soils Geographic Database (STATSGO).

On a daily basis, INFILv3 simulated major components of the mass-balance equation within the unsaturated zone to a depth of 6 m, the depth at which the seasonal effects of ET become insignificant. Net infiltration equaled the sum of snowmelt, precipitation, and infiltrating surface flow minus the sum of ET, runoff, and changes in root-zone storage. Each of these components was estimated on a cell-by-cell basis by using secondary governing equations (Hevesi and others, 2003). Runoff was generated in the model when and where available water exceeded the root-zone storage capacity or the saturated hydraulic conductivity of the soil or bedrock. A surface-water routing process was used to move runoff downstream through a simulated drainage basin and allow the surface water potentially to infiltrate through the root zone.

Net-infiltration simulations were calibrated by fitting the simulated daily discharge from modeled watersheds to stream-flow records at 31 gaged sites in the DVRFS region (fig. C-7). Model fit was evaluated both qualitatively and quantitatively by comparing simulated to measured daily and annual hydrographs. Model calibration was complicated by sparse daily climate records and information regarding stream-channel characteristics and base-flow contributions, the absence of collocated climate stations and stream-gaging stations in a watershed, and the nonuniqueness of model results (Hevesi and others, 2003). To increase the confidence in the net-infiltration estimates, model results were constrained by prior estimates of recharge that were calculated using alternative methods.

The calibrated net-infiltration model (model 1 in Hevesi and others, 2003) was used to simulate daily net infiltration from 1950 through 1999 across the DVRFS model domain (fig. C-8). This period was selected for simulation primarily because of the availability of climate and streamflow records. An average annual net infiltration of 2.8 millimeters (mm) was estimated over the entire model domain by averaging simulated daily net infiltration over the 50-year simulation period. This estimate is less than 2 percent of the average annual precipitation computed for the same period (Hevesi and others, 2003). An annual potential recharge of about 125 Mm³ was computed by multiplying the average annual infiltration by the area of the model domain. Results presented by Hevesi and others (2003) indicate a wide range in the simulated rate of net infiltration across the model domain. Local net-infiltration rates ranged from near zero to a maximum of about 1,262 millimeters per year (mm/yr) beneath a stream channel. The simulated average annual runoff over the 50-year simulation period was 2.2 mm, of which 0.2 mm eventually flowed into lowland playas where it was evaporated or infiltrated into the subsurface (Hevesi and others, 2003). About 14 percent of the total net infiltration simulated over the 50-year period was from overland flow, but locally the overland flow accounted for as much as 40 percent (Hevesi and others, 2003).

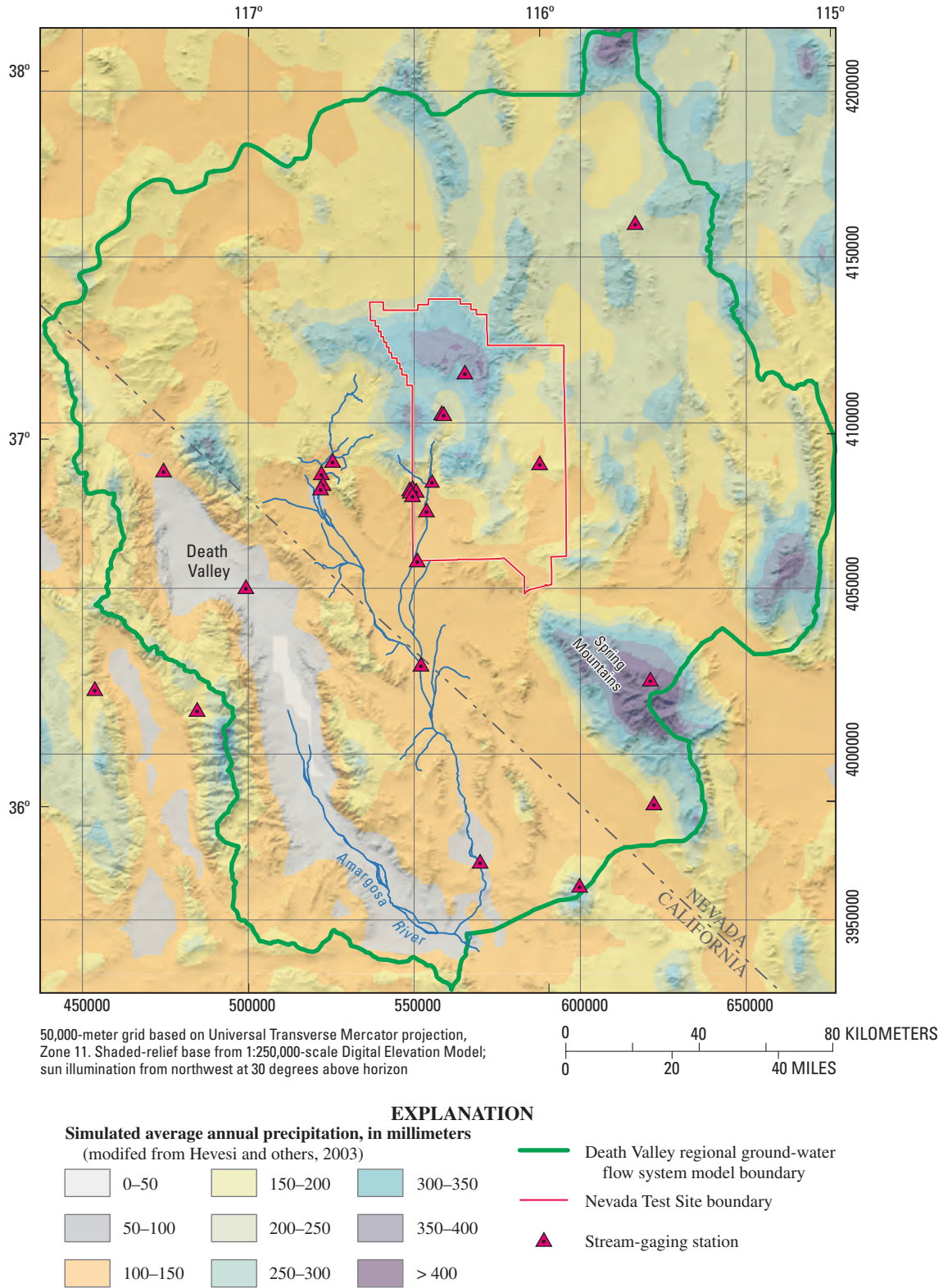
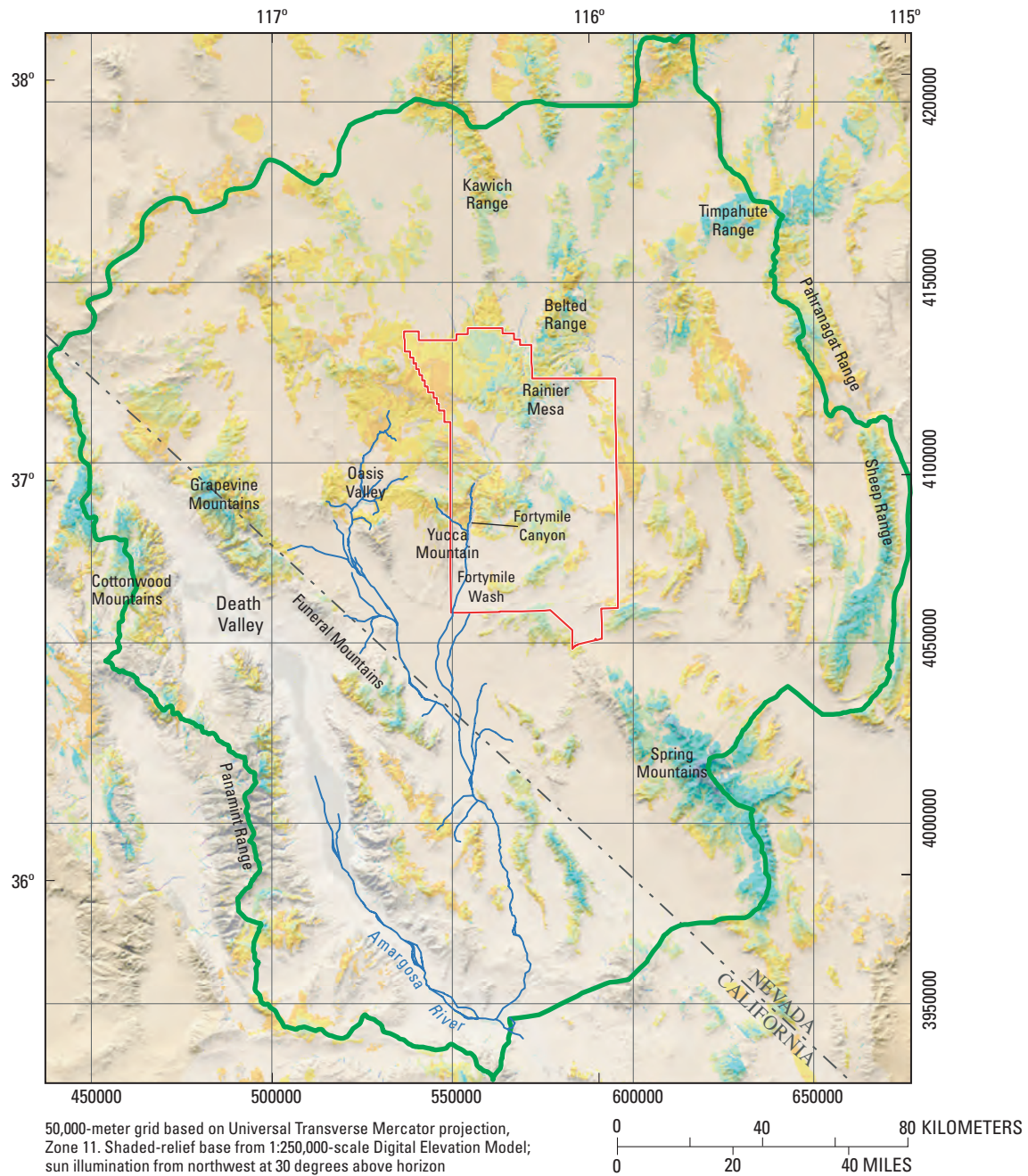


Figure C-7. Simulated average annual precipitation and stream-gaging stations used to calibrate the net-infiltration model in the Death Valley regional ground-water flow system model region.



EXPLANATION

Net infiltration, in millimeters per year (based on model 1 simulation of Hevesi and others, 2003)

0-0.1	5-10	100-500
0.1-1	10-20	> 500
1-2	20-50	
2-5	50-100	

- Death Valley regional ground-water flow system model boundary
- Nevada Test Site boundary

Figure C-8. Simulated net infiltration used to estimate recharge to the Death Valley regional ground-water flow system model region, 1950-99.

Simulated net-infiltration rates, averaged over the period 1950–99, were generally consistent with published (Hevesi and others, 2003, table 1) estimates of recharge in the DVRFS region. The reported annual estimate of recharge from 42 continuous hydrographic areas including most of the DVRFS region was about 157 Mm^3 (Hevesi and others, 2003). The simulated annual net infiltration for this same area was 4 percent less at 151 Mm^3 .

The uncertainty in model-generated net infiltration estimates was related to uncertainties associated with the representation of the near-surface environment and the unsaturated zone processes. Hevesi and others (2003) presented model uncertainty qualitatively because the results of their study could not support a rigorous quantification of uncertainty. Model uncertainty remained high for many model inputs such as bedrock permeability, soil thickness, root density as a function of depth, stream-channel properties, spatial distribution of climate by month (computed from daily records), and potential evapotranspiration coefficients. Although the general magnitude of the simulated net-infiltration volume was consistent with prior discharge and recharge estimates for the DVRFS region, substantial differences were observed in some local basins. Nonetheless, the spatial distribution of estimated net infiltration was considered a reasonable indication of the spatial distribution of the potential recharge across the model domain under current climate conditions (Hevesi and others, 2003).

On the basis of the net infiltration simulated by Hevesi and others (2003), the major areas of the model domain receiving recharge are along the eastern model boundary beneath the Timpahute, Pahrnatag, and Sheep Ranges and the Spring Mountains; along the western part of the model boundary beneath the Panamint Range and Cottonwood Mountains; beneath the Kawich and Belted Ranges and Rainier Mesa, near the northern part of the NTS area; and beneath the Grapevine Mountains and the southern part of the Funeral Mountains, along the eastern margin of Death Valley (fig. C–8). In addition, small concentrated areas of recharge occur beneath major drainages, such as Fortymile Canyon and Fortymile Wash near Yucca Mountain and the Amargosa River near Oasis Valley, and beneath channels draining the Panamint Range and along well-developed drainages that incise major alluvial fans in Death Valley.

Lateral Flow

Areas of potential inflow and outflow, or lateral ground-water flow, along the DVRFS model boundary were defined for prepumped conditions (Appendix 2, this volume). Hydraulic gradients determined from a regional potentiometric map (plate 1 and Appendix 1, this volume) indicate that one boundary segment has no flow and that flow occurs across 11 of 12 lateral boundary segments of the model domain—7 boundary segments have inflow (Eureka and Saline are combined) and 3 have outflow (fig. C–9).

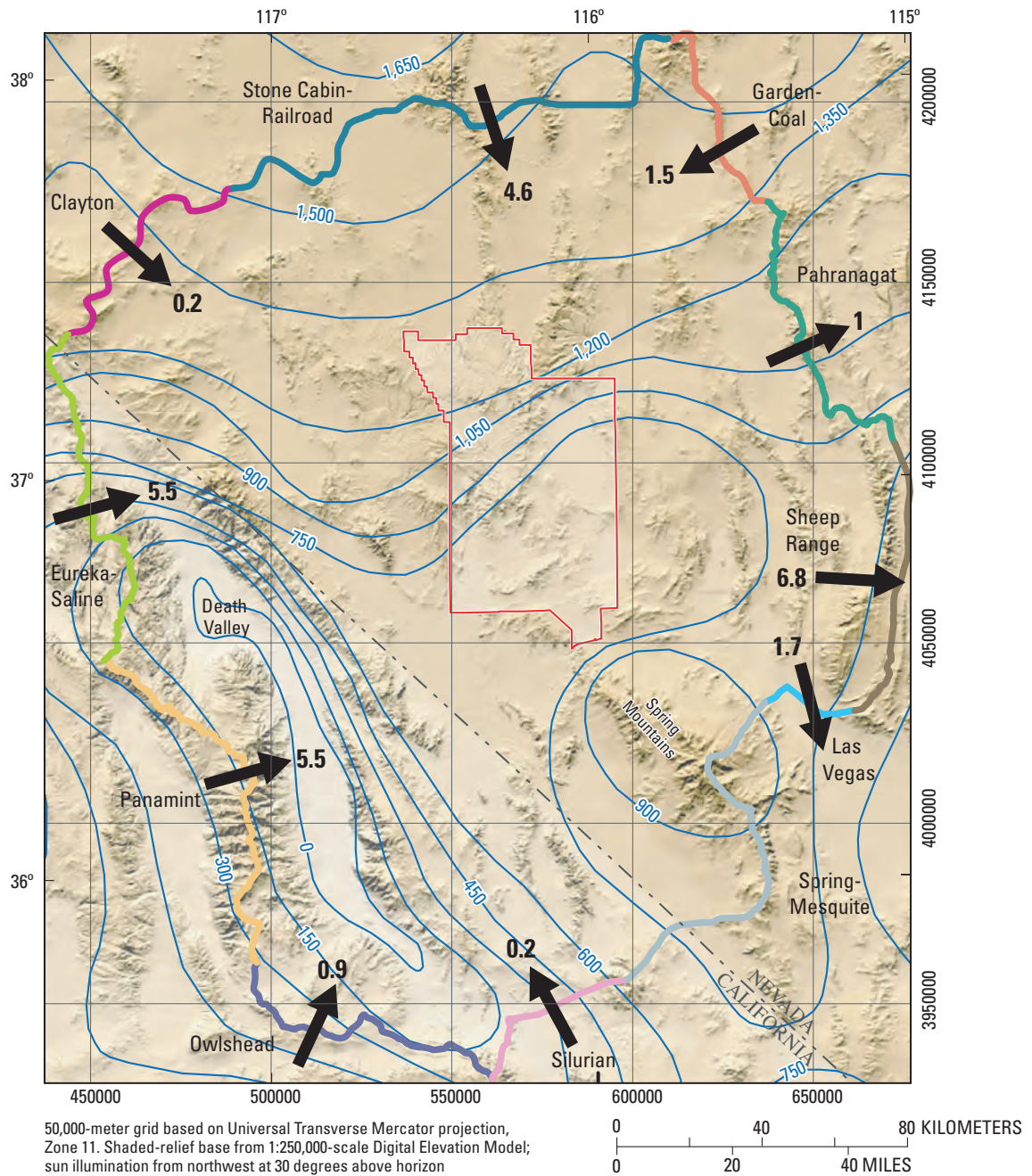
Lateral flow was estimated using the Darcy equation with hydraulic gradients defined by regional water levels, and estimates of hydraulic conductivity and the cross-sectional area of HGUs along the model boundary. Where possible, lateral-flow estimates were constrained by inflows and outflows estimated from available water-budget information for areas adjacent to the model domain. Where discrepancies between Darcy and water-budget flow estimates were great, alternative interpretations of the data, such as local adjustments to the composite hydraulic conductivity or reappraisals of the surrounding area water budgets, were used to further develop a reasonable estimate of lateral-boundary flow for the boundary segment.

Lateral-flow estimates for each boundary segment are given in table C–4. The table includes Darcy and water-budget estimates and the estimate considered most reasonable for prepumped conditions (Appendix 2, this volume). On the basis of these estimates of lateral flow, nearly 18.4 Mm^3 of ground water flows into the model domain annually, primarily along the western and northern parts of the model boundary, and 9.5 Mm^3 flows out, primarily along the eastern part of the model boundary (fig. C–9 and table C–4). The greatest inflow occurs from the area west of Death Valley, and the greatest outflow to the area east of the Sheep Range. The estimated annual net lateral flow is about 8.8 Mm^3 into the model domain.

Balance of Components

The water budget commonly is used to assess the significance of individual flow components in the ground-water system and to evaluate the balance between inflows and outflows. The volumetric flows estimated for the major water-budget components of the DVRFS from data previously presented in this chapter are summarized in table C–5. For prepumped conditions, annual recharge accounted for about 87 percent of the total inflow (143.4 Mm^3), and natural discharge (ET and spring flow) about 93 percent of the total outflow (133.8 Mm^3). The remainder (less than 10 percent) of the inflow and outflow is accounted for by lateral flows into and out of the model domain. The difference between estimated prepumped inflows and outflows is less than 7 percent of the estimated inflow. By 1998, pumpage was about 93.5 Mm^3 , which equates to about 70 percent of the total outflow estimated for prepumped conditions. It should be noted that this pumpage estimate is not adjusted for any potential return flow and that table C–5 does not include return flow as a potential inflow to the 1998 water budget.

Water naturally discharging as spring flow and(or) ET and water stored in pore spaces of subsurface rock units are two likely sources for the ground water pumped from the DVRFS. A decrease in estimated spring discharge—from 16.8 Mm^3 for prepumped conditions to 5 Mm^3 in 1998 (table C–5)—indicates that ground-water pumping has affected natural discharge. The water budget given in table C–5 also indicates that ET in 1998 is likely to be less than that estimated for prepumped conditions and possibly



EXPLANATION

Death Valley regional ground-water flow system model boundary segment

- Lateral-flow boundary—
- Colors delineate segments
- No-flow boundary

1 Lateral flow—Arrow indicates direction; number indicates annual volume in millions of cubic meters from table C-4.

—750— Regional potentiometric-surface contour—
Interval is 150 meters. Datum is sea level.
(Bedinger and Harrill, Appendix 1, this volume)

— Nevada Test Site boundary

Figure C-9. Regional ground-water potentiometric surface and lateral flow across boundary segments of the Death Valley regional ground-water flow model domain.

Table C-4. Estimates of flow across lateral boundary segments of the Death Valley regional ground-water flow system model domain for prepumped conditions.

[+ values, flow into model domain; – values, flow out of model domain; --, no value was reported or estimate was unreliable; m³/d, cubic meter per day; m³, cubic meter]

Boundary segment (shown in fig. C-9)	Boundary flow estimate (m ³ /d)			Estimate of annual boundary flow ¹ (m ³)
	Darcy calculation	Water-budget calculation	Most reasonable estimate	
Silurian	-125	-11,400	500 ²	183,000
Spring-Mesquite	-782	--	0 ³	0
Las Vegas	-4,575	--	-4,575	-1,671,000
Sheep Range	-18,747	--	-18,747	-6,847,000
Pahrnanagat	-2,783	--	-2,783	-1,016,000
Garden-Coal	4,139	--	4,139	1,512,000
Stone Cabin-Railroad	12,476	--	12,476	4,557,000
Clayton	667	--	667	244,000
Eureka-Saline ⁴	20,873	14,600–15,600	15,100	5,515,000
Panamint	14,050	14,000–16,000	15,000	5,479,000
Owlshead	2,382	--	2,382	870,000
Total	27,576		24,193	8,826,000

¹Volume calculated using most reasonable estimate of boundary flow; from data analyses in Appendix 2 (this volume), rounded to the nearest 1,000 m³.

²See Appendix 2 (this volume) for explanation of method used to determine most reasonable estimate.

³No significant flow estimated across boundary because segment closely coincides with natural no-flow boundary.

⁴Estimate is sum of flows across Saline and Eureka boundary segments.

represents a source of natural discharge reduced by local pumpage. Given the relatively short time period (less than a century), this decrease in discharge is probably not due to climatic influences. Accordingly, this interpretation would support a higher estimate of prepumped discharge than that presented in table C-5.

The other potential source of ground water pumped from the DVRFS model domain is water stored in the pores of sub-surface rock. This water, when removed from the flow system, decreases the hydraulic head in the aquifer. Although the actual volume of stored ground water is uncertain, preliminary estimates, based on sparse available data on storage properties, indicate that storage accounts for the largest amount of the available water (Harrill, 1986, p. 18; Dettinger, 1989, p. 22). Measured declines in hydraulic head and only small decreases in spring discharge relative to the total amount of ground water being pumped from the DVRFS strongly indicate that the primary source of water pumped from the DVRFS model domain is stored ground water.

Hydraulic Properties

Belcher and others (2001) compiled published and unpublished hydraulic-property data to estimate hydraulic properties of the major HGUs defined for the DVRFS (see Chapter B, this volume). The hydraulic-property estimates included those for transmissivity, hydraulic conductivity, storage coefficient, and anisotropy ratios. With the exception of the lower clastic-rock confining unit (LCCU), however, only

aquifer tests were used to estimate the hydraulic properties of an HGU. Belcher and others (2001) evaluated these data to characterize the hydraulic properties of the major HGUs. Hydraulic conductivity was the only property with a sufficient number of estimates to generate statistical distributions for specific HGUs. Belcher and others' (2001) compilation provided the data set from which hydraulic properties, primarily hydraulic conductivity, were estimated for the transient flow model. Storage coefficients are not discussed because field data are extremely limited (Harrill, 1986, p. 31; Belcher and others, 2001; Carroll and others, 2003). Consequently, values given in standard hydrogeology textbooks were considered adequate for purposes of this investigation.

Hydraulic Conductivity

Belcher and others (2001) estimated horizontal hydraulic conductivity (hereinafter referred to as hydraulic conductivity) by dividing transmissivity calculated from an aquifer test by the total thickness of the aquifer material being tested. Because an HGU is typically stratified and the individual aquifers or confining units have unknown thicknesses, Belcher and others (2001) used the length of the open interval of the well or borehole as the unit thickness. Belcher and others (2001) indicate that while this simplifying approach is not optimal, it is considered appropriate given the available data and nature of the units tested. This approach also was used in previous regional modeling studies in the DVRFS region (IT Corporation, 1996b).

Table C-5. Annual volumetric flow estimates of major water-budget components of the Death Valley regional ground-water flow system model domain for prepumped conditions and 1998 conditions.

[--, no estimate was made or available; Mm³, millions of cubic meters; ET, evapotranspiration]

Water-budget component	Estimated annual volumetric flow (Mm ³)	
	Prepumped conditions	1998
Inflow		
Recharge (net infiltration)	125	125
Boundary inflow (table C-4)	18.4	--
Total	143.4	
Outflow		
Natural discharge: ET ¹	107.5	³ <107.5
Spring flow ² (table C-2)	16.8	5
Boundary outflow (table C-4)	9.5	--
Pumpage (table C-3)	0	93.5
Total	133.8	
Difference (inflow-outflow)	9.6	
Difference (percent)	6.7	

¹Estimate for prepumped conditions not included in estimate given in table C-1 for Pahrump Valley.

²Bennetts and Manse Springs were reported dry after 1975.

³"Less than" symbol is not intended to quantify discharge, but only to indicate that the component likely is less than the prepumped natural discharge.

Pumping and companion observation wells commonly are constructed in water-producing zones of an HGU in the model domain. Data collected from these wells may represent the more transmissive zones of an HGU; therefore, transmissivities calculated from these data may be biased to larger values. This bias may be compounded further by the assumption that the thickness of a unit is limited to the length of the open interval of the well when calculating hydraulic conductivity. Thus, the means and variances presented by Belcher and others (2001) may be most representative of the hydraulic properties of the more productive zones in an HGU.

Variability inherent in the HGUs across the DVRFS region increases the uncertainty of the estimated hydraulic conductivity values. Lithologic factors, such as facies changes in sedimentary rock, changes in welding in volcanic rock, and degree of fracturing, can cause hydraulic conductivity values to vary substantially over relatively short distances. Variability also can result from sampling bias. Variability for estimates of the matrix permeability commonly depends upon the variable lithology and interval penetrated by the well within a particular unit. Sampling variability also can be a factor in fractured rocks if boreholes intersect rocks with different degrees of fracturing.

Probability Distributions

Data from Belcher and others (2001) were used to estimate probability distributions and to provide reasonable ranges of hydraulic conductivity for the major HGUs in the DVRFS region (Belcher and others, 2002). Fracturing appears to have the greatest influence on the permeability of bedrock HGUs—the greater the degree of fracturing, the greater the permeability. Alteration and welding in the Cenozoic volcanic rocks also greatly influence hydraulic conductivity. Alteration decreases hydraulic conductivity, and welding forms brittle rocks that fracture more easily, thereby increasing hydraulic conductivity. In Chapter B (this volume), these relations are used to establish hydraulic-conductivity zones. Table C-6 presents probability distributions of hydraulic conductivity for the major HGUs in the DVRFS region.

Depth Decay

Intuitively, hydraulic conductivity decreases with depth as the geostatic load increases, compressing favorably oriented fractures, faults, and sedimentary units. Analyses of covariance confirmed the assumption that depth was a significant factor in the variability of hydraulic conductivity in the DVRFS region, but variability in hydraulic-conductivity estimates because of other factors prevents a rigorous quantification of a depth decay function.

The relation between hydraulic conductivity and depth in the DVRFS region has been postulated by Bedinger and others (1989), IT Corporation (1996b), and D'Agnesse and others (1997). Bedinger and others (1989) developed a series of curves defining the distribution of hydraulic conductivity for hydrogeologic units in the region. The hydraulic-conductivity values of each unit were affected by the variation of rock properties by depth and degree of faulting. Using these findings, D'Agnesse and others (1997) indicate qualitatively that the hydraulic conductivity decreases rapidly for most rocks between depths of 300 to 1,000 m across the model domain. At depths greater than 1,000 m, matrix permeability probably dominates, except in regional fault zones. At depths greater than 5,000 m, the geostatic load probably keeps faults and fractures closed (D'Agnesse and others, 1997). The study by the IT Corporation (1996b, p. 29) postulated a relation of exponentially decreasing hydraulic conductivity with depth in the alluvial aquifer (equivalent to the AA and ACU units in table C-6), in the volcanic aquifer (equivalent to part of the Cenozoic volcanic-rock HGUs), and in the lower carbonate-rock aquifer (LCA). Decreasing trends in hydraulic conductivity are evident in the data presented in this study (IT Corporation, 1996b, figs. 6-1, 6-2, and 6-3), despite a great deal of apparent scatter in the data.

On the basis of regression analysis, Belcher and others (2001) found the best relation was between log₁₀-transformed hydraulic conductivity and depth. The logarithmic values of hydraulic conductivity were used for statistical calculations because this parameter tends to be log-normally distributed

Table C-6. Horizontal hydraulic-conductivity estimates of hydrogeologic units in the Death Valley regional ground-water flow system (modified from Belcher and others, 2001; 2002).

[Abbreviations: AA, alluvial aquifer; ACU, alluvial confining unit; BRU, Belted Range unit; CFBCU, Crater Flat–Bullfrog confining unit; CFPPA, Crater Flat–Prow Pass aquifer; CFTA, Crater Flat–Tram aquifer; CHVU, Calico Hills volcanic-rock unit; ICU, intrusive-rock confining unit; LCA, lower carbonate-rock aquifer; LCCU, lower elastic-rock confining unit; LFU, lava-flow unit; OAA, older alluvial aquifer; OACU, older alluvial confining unit; OVU, older volcanic-rock unit; PVA, Paintbrush volcanic-rock aquifer; SCU, sedimentary-rock confining unit; TMVA, Thirsty Canyon–Timber Mountain volcanic-rock aquifer; UCA, upper carbonate-rock aquifer; UCCU, upper elastic-rock confining unit; VSU, volcanic- and sedimentary-rock unit; XCU, crystalline-rock confining unit; YAA, younger alluvial aquifer; YACU, younger alluvial confining unit; YVU, younger volcanic-rock unit; NA, not applicable]

Hydrogeologic unit or subunit	Hydraulic conductivity (meters per day)				95-percent confidence interval	Number of measurements
	Geometric mean ¹	Arithmetic mean	Minimum	Maximum		
AA ²	1.5	10.8	0.00006	130	0.005–430	52
ACU ³	3	10.5	0.003	34	0.02–470	15
LFU	NA	NA	0.002	4	NA	2
YVU & VSU	0.06	1.5	0.00004	6	0.00005–80	15
TMVA	0.01	2	0.0002	20	0.00001–18	11
PVA	0.02	4	0.000007	17	0.0000003–1300	9
CHVU	0.2	0.55	0.008	2	0.007–5	14
BRU	0.3	1.03	0.01	4	0.006–17	6
CFTA	0.05	0.4	0.003	2	0.0004–5.3	11
CFBCU	0.4	6.8	0.0003	55	0.0006–240	34
CFPPA	0.3	13	0.001	180	0.000006–2.4	19
OVU	0.004	0.07	0.000001	1	0.00002–5	46
ICU	0.01	0.3	0.0006	1.4	0.00002–5	7
SCU	0.002	0.02	0.0002	0.3	0.00004–0.09	16
UCA & LCA	2.5	90	0.0001	820	0.0008–7700	53
fractured	19	150	0.01	820	0.03–11,000	32
unfractured	0.1	1.6	0.0001	14	0.0002–70	21
UCCU & LCCU ⁴	0.00002	0.2	3×10 ⁻⁸	5	1×10 ⁻¹⁰ –3	29
shale	0.01	0.07	0.0002	0.4	0.0001–1.4	9
quartzite	0.000001	0.24	3×10 ⁻⁸	5	1×10 ⁻¹⁰ –0.006	19

¹Values determined from log-transformed distribution.

²AA is the combined YAA and OAA.

³ACU is the combined YACU and OACU.

⁴One measurement could not be classified as shale or quartzite.

(Neuman, 1982). The Cunnane plotting position method was used to assess the normality of the logarithms of hydraulic-conductivity estimates for each major HGU (Helsel and Hirsch, 1992, p. 27–29). In most cases, the assumption of a normal distribution for log hydraulic conductivity was true.

For the major HGUs, 14 of the 15 relations between depth and log hydraulic conductivity had a correlation coefficient that ranged from virtually zero to 0.52. Depth and log hydraulic conductivity possibly are correlated for the Belted Range unit ($r^2=0.78$), although the regression was determined with only six data pairs.

Despite poor results from the regression analysis, a relation between depth and hydraulic conductivity might exist at the scale of this investigation. Hydraulic-conductivity estimates were available only to depths of less than 3,600 m, and the average depth investigated was only 700 m. A possible relation between depth and hydraulic conductivity could be investigated further through calibration of regional models.

Hydraulic Head

Hydraulic-head measurements at each measurement site were composited to develop hydraulic-head observations. Errors in well altitude and location, nonsimulated transient stress, and water-level measurement were estimated to quantify the uncertainty of the head observations.

Head Observations

Periodic depth-to-water measurements and continuous down-hole water pressure measurements made in wells throughout the DVRFS model domain were used to develop hydraulic-head observations. The observations for each well, which composite one or more water-level measurements, were used in calibrating the ground-water flow model. These data were acquired as part of activities associated with many historical and currently active water-level monitoring networks,

each of which was established to address a specific interest in a study area. Active monitoring networks include those funded or operated by Nye County, the States of Nevada and California, U.S. Geological Survey, National Park Service, U.S. Fish and Wildlife Service, and the U.S. Department of Energy Yucca Mountain Project and Underground Test Area Program. Much of these data and other water-level information available from local mining operations have been included in the U.S. Geological Survey's National Water Information System (NWIS). NWIS, specifically its ground-water component, the Ground-Water Site Inventory (GWSI), served as the primary source and repository for water levels and associated borehole information used to develop and calibrate the DVRFS ground-water flow model. Temporal and spatial gaps in water-level data were evaluated and, where possible, addressed by making additional measurements and by entering any previously omitted water-level information into the GWSI.

The GWSI, although comprehensive and complete in terms of water-level measurements and borehole and well information, has limited options for assigning ancillary information to individual water-level measurements. Thus, a project database was designed to retrieve site, construction, borehole, and water-level information directly from GWSI and store additional information about each water-level measurement.

Ancillary information about each water level was incorporated into the project database by assigning attributes. This information included one general-condition attribute and multiple detailed-condition attributes for each water-level measurement (table C-7). The general-condition attribute indicates the appropriateness of the measurement as a steady-state or transient head observation. The detailed-condition attribute provides additional information about the condition or state of the measurement or of the well at the time the measurement was made.

The general-condition attribute identifies measurements determined acceptable as head observations for calibration of the regional ground-water flow model. Measurements representative of regional ground-water conditions were identified as regional-scale measurements. All other general-condition attributes indicate that the measurement is unacceptable for developing head observations for calibration of the regional ground-water flow model. These regional measurements were attributed as either steady state or transient. A regional transient designation is assigned only to those water levels in which the measured response is considered to be the result of ground-water pumpage. Detailed-condition attributes provide information to support the general condition assigned to the measurement. These attributes include information about the condition and location of the well, observed trends in the water level, and reported and likely explanations for measured water-level changes.

Attributes assigned to each category were determined by analyzing hydrographs, reviewing reports pertaining to water levels measured nearby, and evaluating the well location relative to centers of pumping and underground nuclear tests. Reports include mainly those published as part of previously

mentioned monitoring networks. Open-interval depth information for wells also was evaluated to assess whether measured fluctuations result from precipitation variations or evapotranspiration. Measurements from wells having insufficient information from which to determine or estimate an open interval were not used to develop head observations. This attributing procedure is illustrated by an annotated hydrograph of water levels from a well in Pahrump Valley (fig. C-10).

Nearly 40,000 water levels measured in about 2,100 wells were evaluated in the model domain. Of these, about 12,000 water levels in 700 wells were assigned attributes indicating that the water level represented regional, steady-state conditions. Head observations for calibration of prepumped conditions were computed at each of the 700 wells as the average of all measurements attributed as representing regional, steady-state conditions. The spatial distribution of the 700 steady-state head observations is shown in figure C-11. Head observations range from about 2,500 m above sea level in the Spring Mountains to nearly 100 m below sea level in Death Valley. In general, head decreased from north to south. Local areas of higher head are coincident with mountainous areas where regional aquifers receive recharge from precipitation.

Nearly 15,000 water levels measured in about 350 wells were attributed to indicate that the measurements represented regional, transient (pumped) conditions (fig. C-12). These measurements, along with those attributed as regional steady-state water-level measurements, were used to develop the set of transient-head observations used to calibrate the ground-water flow model. Water-level records for individual wells spanned periods from 1 to about 50 years. Water levels attributed as representing regional steady-state or transient conditions were averaged by year and by well to compute the almost 5,000 head observations used to calibrate the transient ground-water flow model.

The earliest reported water level usable for the DVRFS ground-water flow model was measured in 1907. Most wells having longer term water-level records are in Pahrump Valley (fig. C-12). Nearly 100 wells in the DVRFS model domain have a record of 20 years or longer. The greatest drawdown measured in the DVRFS model domain is 76 m, which was measured in a well in the Beatty area just north of Amargosa Desert (fig. C-12). Most wells have less than 15 m of measured drawdown; wells having the greatest drawdown (>15 m) typically are in areas of concentrated irrigation use, primarily the Amargosa Desert and Pahrump and Penoyer Valleys (fig. C-12).

Every well in which a water level was measured was attributed to indicate the depth of the interval contributing water to the well. Two depth attributes were assigned to each well—one representing the top of the uppermost open interval, and the other, the bottom of the lowermost open interval. Depth attribute values were determined from well-construction and borehole information stored in GWSI. For wells in which specific screen- or open-interval information was not known, top and bottom interval values were estimated from reported well depths, hole depths, casing information, and water levels.

Table C-7. Description of attributes assigned to water levels retrieved from Ground-Water Site Inventory (GWSI) for simulation of ground-water flow in the Death Valley regional ground-water flow system model domain.

General-condition attribute		
Attribute name	Description	Considered appropriate for regional evaluation
Duplicate	Measurement entered under another site identifier.	NO
Insufficient data	Measurement does not have sufficient supporting information to determine general condition.	NO
Localized	Measurement represents localized hydrologic conditions.	NO
None	Water level not measured because well was dry or obstructed.	NO
Nonstatic level	Measurement affected by sampling, testing, construction, or some other local activity.	NO
Steady state-LOCAL	Measurement represents prepumped, equilibrium conditions in a local-scale flow system.	NO
Steady state-REGIONAL	Measurement represents prepumped, equilibrium conditions in regional ground-water flow system.	YES
Superseded	Measurement replaced by another that more accurately represents ground-water conditions at the site.	NO
Suspect	Measurement is erroneous or affected by unnatural conditions.	NO
Transient-LOCAL	Measurement reflects transient conditions in or near borehole.	NO
Transient-REGIONAL	Measurement reflects changes caused by pumping from the regional ground-water flow system.	YES
Detailed-condition attribute		
Attribute name	Description	
Erratic/Unstable	Measurement appears to be erratic and unstable.	
Evapotranspiration response	Measurement appears to be responding to evapotranspiration.	
Flowing	Measurement is above land surface. In some cases an accurate water level could not be determined due to flowing conditions.	
Insufficient data	Measurement does not have sufficient information to determine detailed conditions.	
Limited data	Measurement is one of a limited number, but general condition is assumed to represent regional conditions.	
Missing	Measurement not assigned a value.	
No date	Measurement not associated with a date.	
Obstruction	Measurement not assigned a value because of an obstruction in borehole.	
Nuclear test effect	Measurement appears to be responding to nearby nuclear test (1951-92).	
Not adjusted for temperature	Measurement not adjusted for a reported temperature effect.	
Precipitation response	Measurement appears to be responding to a recent precipitation event.	
Pumping area	Site is located in an area that may have been affected by ground-water pumping.	
Pumping steady state	Measurement appears to represent steady- or near steady-state conditions during sustained pumping.	
Pumping/recovery	Measurement appears to be responding to pumping in the borehole or in a nearby borehole.	
Reported perched water	Measurement is reported to represent local perched-water conditions.	
Rising trend	Measurement appears to be part of a discernible, overall, rising trend. Possible causes include decrease in nearby pumping and a local precipitation event.	
Seasonal pumping	Measurement appears to be responding to nearby seasonal pumpage.	
Suspect	Measurement is suspect.	
Suspected perched water	Measurement assumed to represent local perched-water conditions.	
Testing area	Well located in area of past nuclear testing.	
Undeveloped	Well not sufficiently developed.	

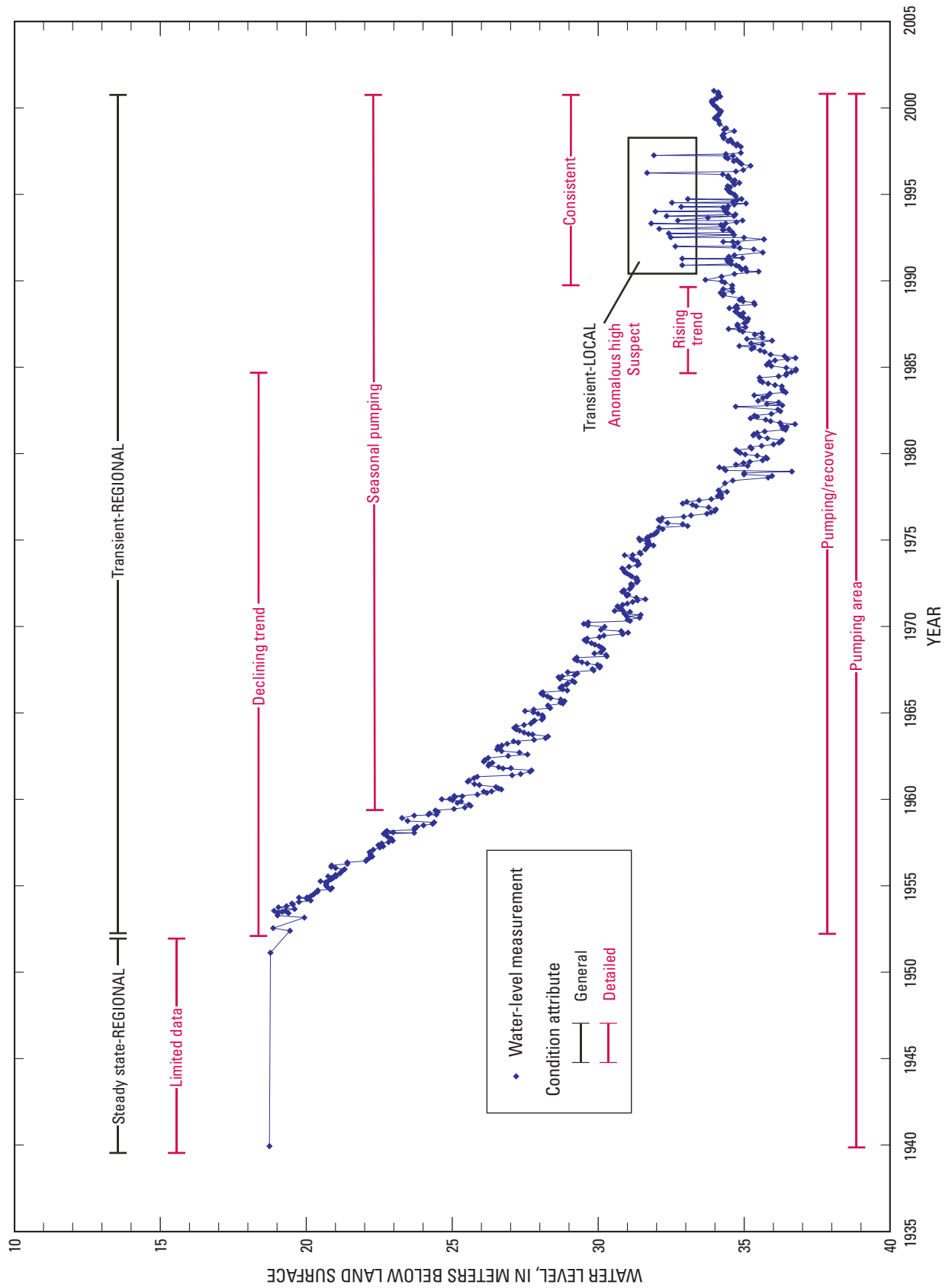
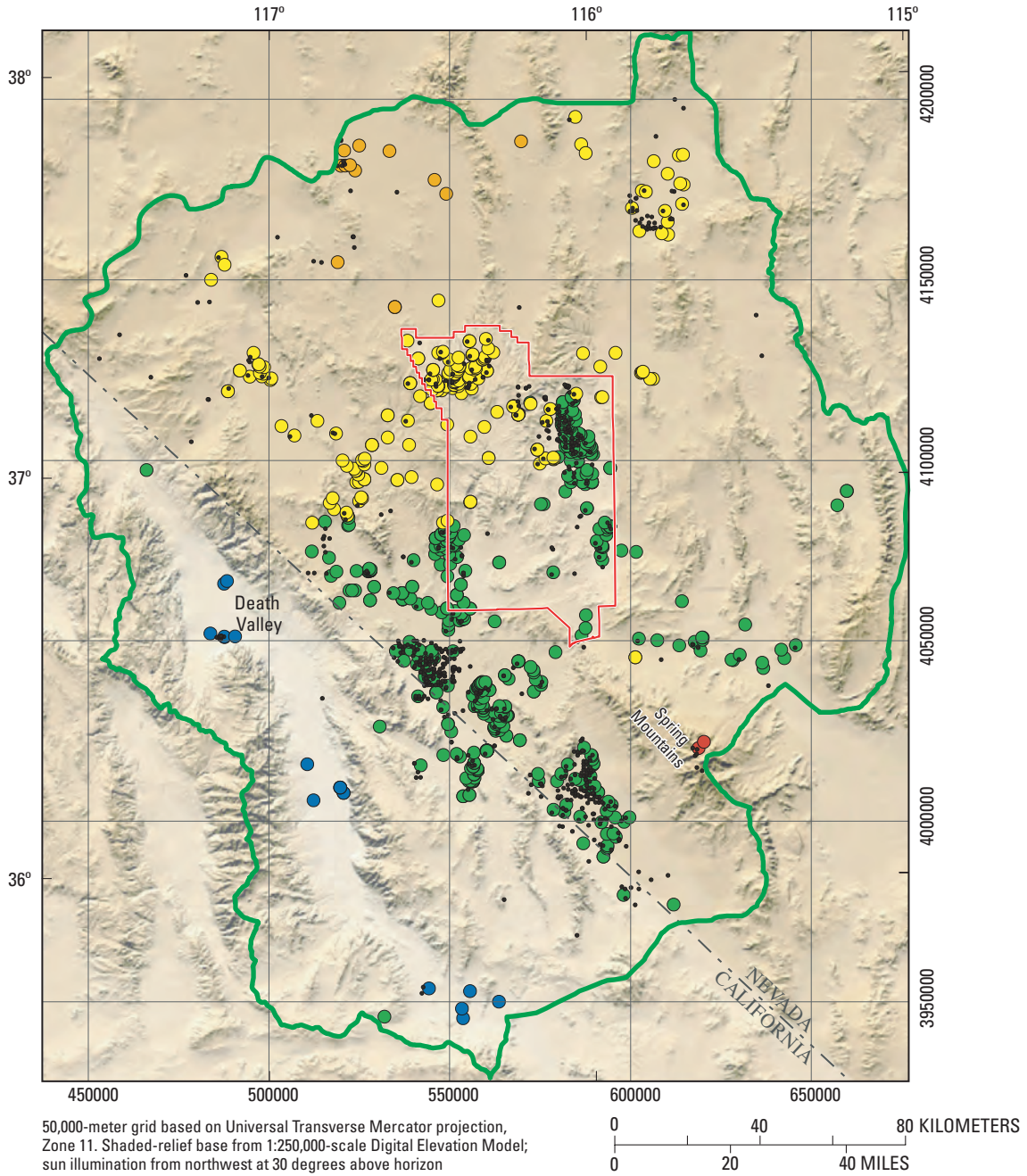


Figure C-10. Annotated hydrograph showing general- and detailed-condition attributes assigned to water-level measurements from a well in Pahrump Valley.



EXPLANATION

- Death Valley regional ground-water flow system model boundary
 - Nevada Test Site boundary
 - Water-level measurements not representative of regional, steady-state conditions
- Head-observation altitude in well representing regional, steady-state conditions—In meters above sea level**
- < 500
 - 500–1,000
 - 1,000–1,500
 - 1,500–2,000
 - 2,000–2,500

Figure C-11. Spatial distribution and altitude of head observations in wells representing regional, steady-state conditions used in calibration of the Death Valley regional ground-water flow system model.

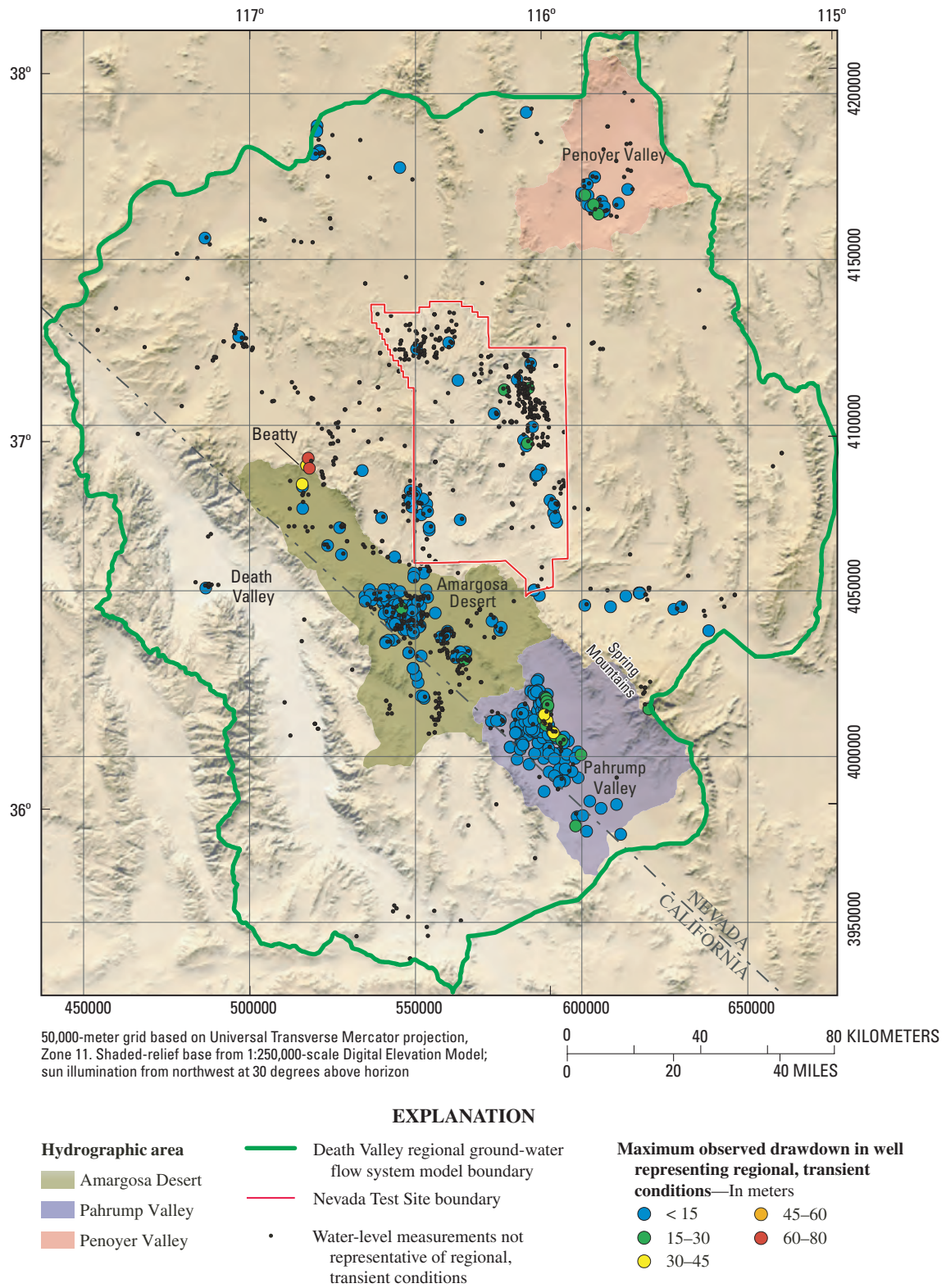


Figure C–12. Spatial distribution and maximum drawdown of head observations in wells representing regional, transient conditions used in calibration of the Death Valley regional ground-water flow system model.

As previously stated, measurements from wells for which information was insufficient to determine or estimate an open interval were not used to calibrate the transient ground-water flow model. Wells used to calibrate the transient flow model are summarized in table C-8. The table lists wells in depth ranges based on the depth of the bottom of the open interval. About 43 percent of the wells have open intervals at depths less than 100 m, and less than 10 percent at depths greater than 1,000 m. The spatial distribution of wells with shallow and deep openings is shown in figure C-13. Most wells having deeper openings are in or near the NTS. The typical depth of the open interval of wells in major agricultural areas of the DVRFS model domain (Amargosa Desert and Penoyer and Pahrump Valleys) is less than 100 m.

Head-Observation Uncertainty

Errors that contribute most to the uncertainty of head observations are associated with potential inaccuracies in the altitude and location given for a well and in the measurement of a water level, and fluctuations introduced by variations in climate or any other nonsimulated transient stress. These errors were estimated from available information and were used to quantify the uncertainty of a head observation.

Table C-8. Bottom depth of open interval for wells used to calibrate the Death Valley regional ground-water flow system model.

[≤, less than or equal to]

Bottom depth of open interval (meters)	Number of wells	Percentage of wells
≤100	369	42.5
≤500	642	74.
≤1,000	803	92.5
≤5,000	868	100.

Well-Altitude Error

Well-altitude error directly affects the calculation of the hydraulic head as referenced to a common datum. The error associated with the potential inaccuracy in well altitude was computed from the altitude accuracy code given in GWSI, expressed as a plus/minus (\pm) range related directly to the method by which the altitude was determined. This range varies from ± 0.03 m for high-precision methods, such as spirit level and differential global positioning system (GPS) surveys, to ± 25 m for estimates determined from topographic maps having large (50 m) contour intervals. The range defined by the altitude accuracy code is assumed to represent, with 95 percent confidence (two standard deviations), the true well-altitude uncertainty. Assuming that the head observation represents the mean value and that the error is normally distributed,

the uncertainty of the head observation, with respect to the well-altitude error, can be expressed as a standard deviation by the following equation:

$$sd = AAC / 2 \quad (1)$$

where

sd is the standard deviation,

and

AAC is the value of the GWSI altitude accuracy code, in meters.

Accordingly, the standard deviation for well-altitude error could range from 0.015 to 12.5 m.

Well-Location Error

Well-location errors can cause a discrepancy between observed and simulated heads. The magnitude of this discrepancy depends directly on the hydraulic gradient at the well—the steeper the gradient, the greater the discrepancy. Well-location error was calculated as the product of the distance determined from the coordinate accuracy code values given in GWSI and the hydraulic gradient estimated for a given well location. Latitude and longitude coordinate accuracy codes given for wells in the DVRFS range from about 0.1 to 100 seconds. In the DVRFS region, a second represents about 33 m. Accordingly, the largest distance accuracy that could be computed for a well in the DVRFS model domain would be about $\pm 3,300$ m. The hydraulic gradient at a well was estimated from a regional potentiometric surface map developed by D'Agnesse and others (1998). The largest gradient estimated from their map was nearly 15 percent and the smallest about 2 percent. The range defined by the value of the coordinate accuracy code is assumed to represent, with 95 percent confidence (or two standard deviations), the true error in the head observation as related to well-location uncertainty. Assuming that the head observation represents the mean value and that the error is normally distributed, the uncertainty of the head observation, with respect to the well-location error, can be expressed as a standard deviation calculated by the following equation:

$$sd = (CAC / 2) \times HG, \quad (2)$$

where

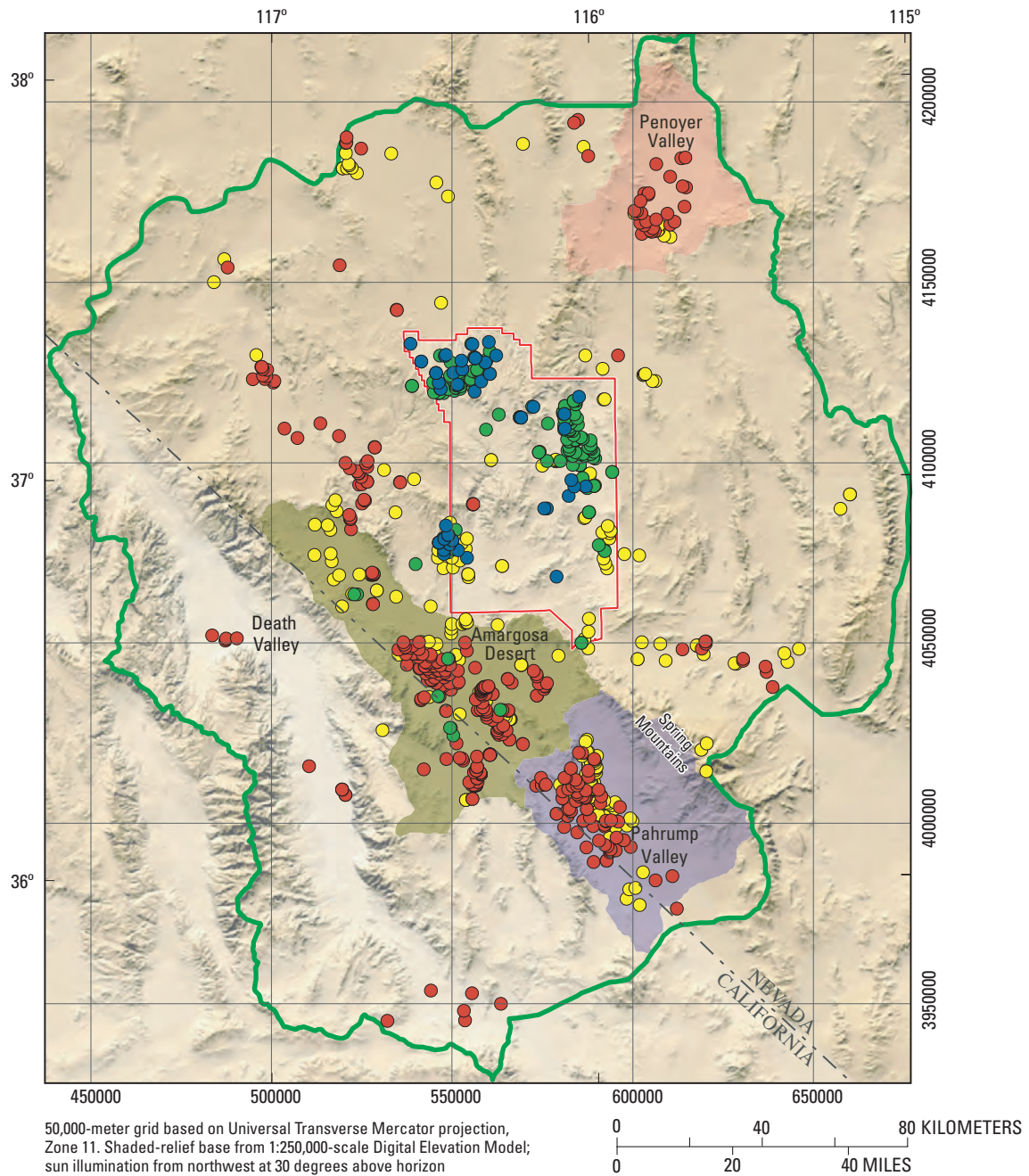
sd is the standard deviation;

CAC is the value of the GWSI coordinate accuracy code, in meters;

and

HG is hydraulic gradient, in percent slope divided by 100.

Accordingly, the standard deviation for well-location error could range from about 0.03 to 250 m.



EXPLANATION

- | | | |
|--------------------------|---|--|
| Hydrographic area | Death Valley regional ground-water flow system model boundary | Bottom depth of opening in head-observation well—In meters below land surface |
| Amargosa Desert | Nevada Test Site boundary | ≤100 |
| Pahrump Valley | | >500 ≤ 1,000 |
| Penoyer Valley | | >100 and ≤ 500 |
| | | >1,000 ≤ 5,000 |

Figure C-13. Spatial distribution and bottom depth of opening in head-observation wells (steady-state and transient conditions) used in calibration of the Death Valley regional ground-water flow system model.

Nonsimulated Transient Error

Nonsimulated transient errors result from uncertainty in the magnitude of water-level response caused by stresses not simulated in the flow model, which are typically seasonal and long-term climate changes. Seasonal water-level fluctuations of nearly 5 m have been measured in shallow wells in the DVRFS model domain. These seasonal fluctuations decrease as the depth of the open interval increases. The quantification of uncertainty associated with seasonal fluctuations in the water level requires a sufficient number of measurements made over an entire year. For observations computed with less than 7 measurements per year, the seasonal fluctuation was set to 5 m for wells with open intervals less than 15 m below land surface and 1.5 m for open intervals greater than 15 m below land surface. For observations computed from seven or more measurements per year, the fluctuation is computed as the difference between the highest and lowest water-level measurement. It was assumed that if at least seven measurements were made per year, then these measurements spanned the entire year.

The long-term climatic response in the water-level record is much more difficult to discern and commonly is masked by pumping effects. On the basis of an analysis of available water-level data, long-term climatic response is relatively small throughout the DVRFS region (less than 1.5 m). The potential error associated with long-term climate response at a well was not calculated independently but instead was accounted for by adding 1 m to the seasonal fluctuation assigned to each well. The range defined by this sum is assumed to represent, with 95-percent confidence (or two standard deviations), the true error in the head observation as related to nonsimulated transient uncertainty. Assuming that the head observation represents the mean value and that the error is normally distributed, the uncertainty of the head observation, with respect to the nonsimulated transient error, can be expressed as a standard deviation calculated by the following equation:

$$sd = (SF + LTC) / 4, \quad (3)$$

where

sd is the standard deviation;

SF is seasonal fluctuation as defined by water-level measurements, in meters;

and

LTC is the long-term climate trend defined as 1 m.

Accordingly, the maximum standard deviation for nonsimulated transient error is 1.5 m for wells having less than 7 measurements and an open interval within 15 m of land surface, and 0.625 m for deeper wells.

Measurement Error

Measurement errors result from inaccuracies in the measurement of the depth to water. Measurement accuracy depends primarily on the device being used to make the

measurement. Typically, the accuracies of measurement devices are less than a meter and are defined as a percentage of the depth of the measurement—the deeper the depth-to-water measurement, the greater the potential error. Errors associated with most devices used to measure water levels in the DVRFS region are described in a standard operating procedure report for water-level measurements at the NTS (U.S. Geological Survey, Las Vegas, Nev., written commun., 2001). The greatest error associated with any of these devices equates to about ± 1 m per 1,000 m or 0.1 percent. Water-level depths measured in the region range from near land surface to about 750 m below land surface. A value computed as 0.1 percent of the water-level measurement was used to represent the potential error in measurement accuracy. The range defined by this value is assumed to represent, with 95-percent confidence (or two standard deviations), the true error in the head observation as related to measurement uncertainty. Assuming that the head observation represents the mean value and that the error is normally distributed, the uncertainty of the head observation, with respect to the measurement-accuracy error, can be expressed as a standard deviation calculated by the following equation:

$$sd = (DOOBS \times 0.001) / 2, \quad (4)$$

where

sd is the standard deviation,

and

$DOOBS$ is depth of the observation, in meters above or below land surface.

Accordingly, the standard deviation for the measurement-accuracy error could range from near 0 to 0.375 m.

Total Head-Observation Error

The potential error associated with each head observation is the composite of all errors contributed by the different sources. This uncertainty, expressed as a standard deviation, was computed as:

$$(sd_1^2 + sd_2^2 + sd_3^2 + sd_4^2)^{1/2}, \quad (5)$$

where

sd_1 is standard deviation of well-altitude error,

sd_2 is standard deviation of well-location error,

sd_3 is standard deviation of nonsimulated transient error,

and

sd_4 is standard deviation of measurement-accuracy error.

Accordingly, the standard deviations representing the uncertainty of head observations used to calibrate steady-state (pre-pumped) conditions generally range from less than 1 to about 40 m (fig. C-14A). About 95 percent of the head observations had an uncertainty of less than 10 m and nearly

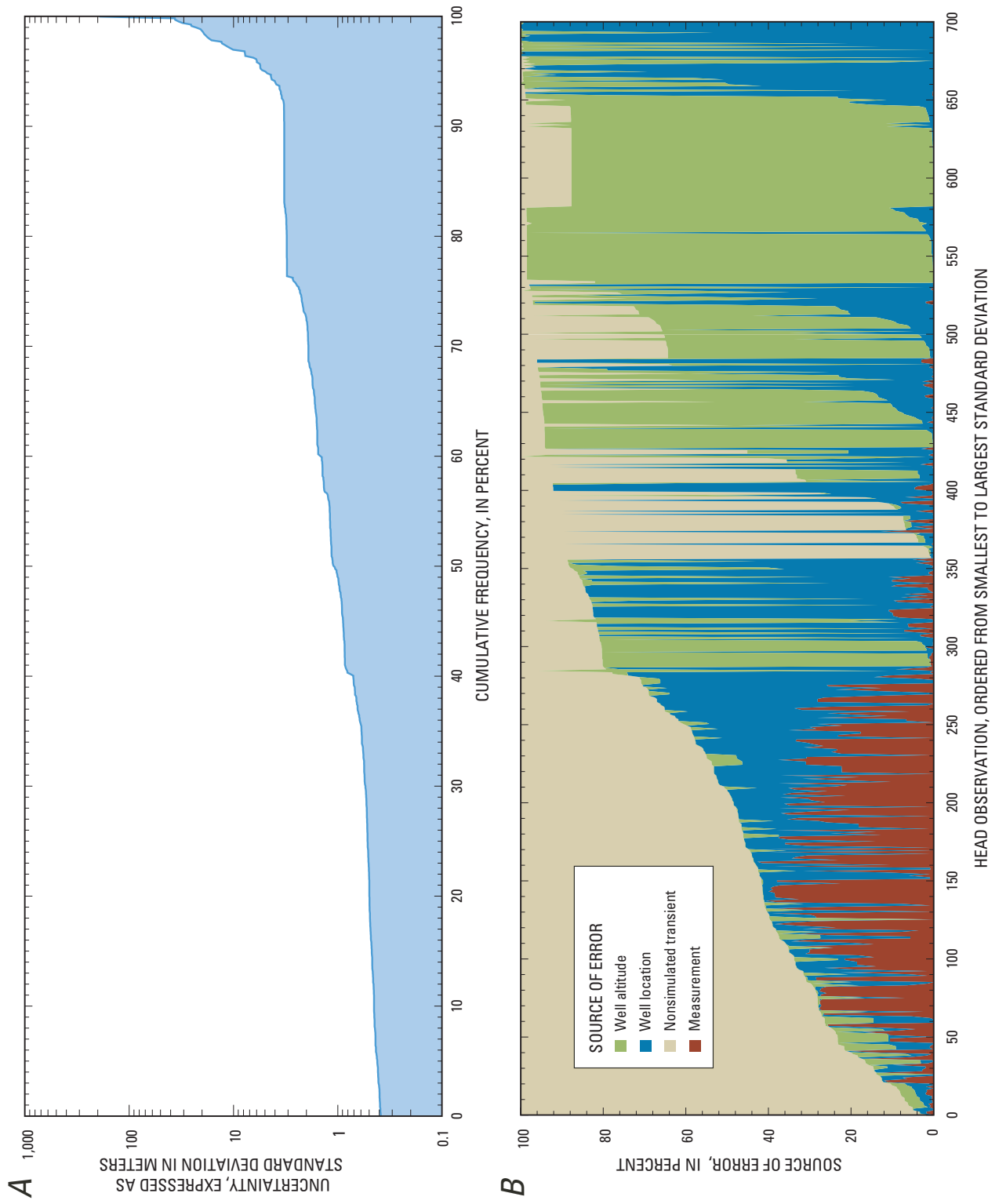


Figure C-14. Uncertainty of 700 head observations computed to represent prepumped, steady-state conditions in the Death Valley regional ground-water flow system model domain.

50 percent had an uncertainty of less than 1 m. The contribution of individual sources to head observation uncertainty varies; but in general, smaller uncertainties were dominated by nonsimulated transient and measurement errors and larger uncertainties by well-altitude and well-location errors (fig. C-14B).

Summary

Information from a series of investigations was compiled to conceptualize and quantify hydrologic components of the ground-water flow system in the Death Valley regional ground-water flow system (DVRFS) model domain and to provide hydraulic-property and head-observation data to be used in the calibration of the transient-flow model. These studies, completed as part of the overall DVRFS investigation, reevaluated natural ground-water discharge occurring through evapotranspiration (ET) and spring flow; the history of ground-water pumping from 1913 through 1998; ground-water recharge simulated as net infiltration; model boundary inflows and outflows based on regional hydraulic gradients and water budgets of surrounding areas; hydraulic conductivity and its relation to depth; and water levels and their appropriateness for regional simulation of prepumped and pumped conditions in the DVRFS model domain. Results appropriate for the regional extent and scale of the model were provided by acquiring additional data, by reevaluating existing data using current technology and concepts, and by refining interpretations using new analyses or algorithms.

Estimates of natural ground-water discharge were evaluated for Death Valley, Oasis Valley, and the other major discharge areas in the DVRFS model domain. Natural ground-water discharge was estimated from evaporation from open water and moist, bare soil and from transpiration by the phreatophytes growing in the discharge area. Discharge from the many regional springs in these discharge areas was accounted for because most spring flow eventually is evapotranspired. In Pahrump and Penoyer Valleys, where ground water is discharged both naturally and by pumping, natural discharge estimates were based on published sources and were assumed to vary with local pumping. In discharge areas not affected by pumping, rates of natural ground-water discharge were assumed to remain fairly constant, presuming no major changes in climate. Mean annual discharge from ET for the model domain is estimated at about 115.5 million cubic meters (Mm^3).

The ET investigations did not account for spring flow where springs supported narrow bands of riparian habitat along the valley margins or where local pumping had decreased spring flow. Previously published spring-discharge rates and some additional measurements of discharge from selected springs were compiled. Annual natural discharge from springs not accounted for in ET studies is estimated at about 16.8 Mm^3 .

The composite annual discharge from Bennetts and Manse Springs, the largest springs in Pahrump Valley, is estimated at 12 Mm^3 prior to ground-water pumping. The local pumping of ground water for large-scale agricultural use in Pahrump Valley caused Bennetts Spring to stop flowing in 1959 and Manse Spring to stop flowing around 1977.

A history of ground-water use for the DVRFS region (1913–98) was developed by compiling available information and using various estimation methods to fill gaps where data were missing. In 1913, ground water used to support agriculture in Pahrump Valley was estimated at less than 5 Mm^3 . Ground-water pumping remained relatively constant through 1944 and thereafter increased steadily in response to agricultural expansion. The estimated total volume of ground water pumped from the DVRFS model domain for the period 1913–98 is about 3,276 Mm^3 and in 1998 about 93.5 Mm^3 . These estimates are not adjusted for water potentially returned to the ground-water flow system.

Recharge in the DVRFS region was estimated from net infiltration using a deterministic mass-balance method. The approach simulated daily climate changes and numerous near-surface processes controlling infiltration. The net-infiltration model, INFILv3, was calibrated to available surface-water flow measurements and constrained by prior estimates of recharge and discharge. The INFILv3 model simulated a mean annual potential recharge to the model domain of about 125 Mm^3 for the period 1950–99.

Lateral flow across the boundary of the DVRFS model domain was estimated. Flows from water-budget studies were compared to those computed by Darcy calculations by using hydraulic gradients obtained from a regional potentiometric-surface map (Appendix 1) and estimated hydraulic conductivities of the hydrogeologic units (HGUs) along the model boundary. The estimated mean annual ground-water flow into the model domain is about 18.4 Mm^3 and out of the model domain is about 9.5 Mm^3 .

A water budget for the prepumping period (pre-1913) computed for the DVRFS model domain was balanced to within about 7 percent. For prepumped conditions, annual recharge accounted for about 87 percent of the total inflow, and natural discharge (ET and spring flow) about 93 percent of the total outflow. Although natural discharge by ET was assumed to represent prepumped conditions, actual discharge may have been reduced some by local pumpage. The remainder of the inflow and outflow is accounted for by lateral flows into and out of the model domain.

The water budget for pumped conditions for the DVRFS model domain is incomplete because accurate estimates for the major hydrologic components are not available. Pumpage in 1998 was about 70 percent of the total outflow estimated for prepumped conditions. A likely source of most of the water being pumped from the DVRFS region is ground water in storage. This water, when removed from the flow system, potentially decreases the hydraulic head within aquifers and decreases natural discharge through ET and from spring flow.

These decreases are partly reflected by declining water-level measurements in areas of pumping and by estimates showing declining spring discharge in Pahrump Valley.

Previously developed reasonable ranges of hydraulic properties, primarily horizontal hydraulic conductivity, were used for the major HGUs of the DVRFS region. Fracturing appears to have the greatest influence on the permeability of bedrock HGUs—the greater the degree of fracturing, the greater the permeability. In the Cenozoic volcanic rocks by alteration decreases hydraulic conductivity, and welding forming brittle rocks that fracture more easily, increases hydraulic conductivity. Storage coefficients from the literature were used because field data necessary to develop HGU-specific values were extremely limited.

The average depth represented by hydraulic-conductivity estimates for the model domain is 700 m with a maximum depth of 3,600 m. Using these limited data, hydraulic conductivity decreased with depth. A rigorous quantification of a depth-decay function was prevented by the variability in available hydraulic-conductivity data.

Nearly 40,000 water levels measured since 1907 in about 2,100 wells were evaluated as part of the DVRFS investigation. Almost 100 wells in the DVRFS model domain have a record of 20 years or longer. Most wells having 30 or more years of water-level record are in Pahrump Valley. About 43 percent of the wells have openings at depths less than 100 m, and less than 10 percent at depths greater than 1,000 m. Wells having deeper openings are generally in or near the NTS. The depth of the open interval for wells in major areas of ground-water pumping (Amargosa Desert and Penoyer and Pahrump Valleys) is typically less than 100 m.

Head observations representing steady-state, prepumped conditions were computed from about 12,000 water levels averaged at 700 wells in the DVRFS model domain. Head observations range from about 2,500 m above sea level in the Spring Mountains to nearly 100 m below sea level in Death Valley. Transient, pumped conditions were represented by head observations computed from nearly 15,000 water levels measured in about 350 wells. Water-level records for individual wells spanned periods from 1 to about 50 years. Most wells have less than 15 m of measured drawdown. Wells having measured drawdown greater than 15 m typically are in areas of concentrated irrigation use, primarily the Amargosa Desert and Pahrump and Penoyer Valleys. The largest drawdown is 76 m, which was measured in a well located in the Beatty area just north of the Amargosa Desert.

Each head observation was assigned an uncertainty based on potential errors related to uncertainties in the altitude and location given for a well, potential inaccuracies in the measurement of a water level, and fluctuations introduced by variations in climate or any other nonsimulated transient stress. The uncertainty of each head observation was represented by a standard deviation calculated by compositing the individual source errors. Standard deviations representing the uncertainty of the head observations range from less than 1 to about 200 m with only one observation having an uncertainty exceeding 40 m.

References Cited

- Ball, S.H., 1907, A geologic reconnaissance in southwestern Nevada and eastern California: U.S. Geological Survey Bulletin 308, 218 p., 3 plates.
- Bedinger, M.S., Langer, W.H., and Reed, J.E., 1989, Hydraulic properties of rocks in the Basin and Range province, *in* Bedinger, M.S., Sargent, K.A., Langer, W.H., Sherman, F.B., Reed, J.E., and Brady, B.T., Studies of geology and hydrology in the Basin and Range province, southwestern United States, for isolation of high-level radioactive waste—Basis of characterization and evaluation: U.S. Geological Survey Professional Paper 1370–A, p. 16–18.
- Belcher, W.R., Elliott, P.E., and Geldon, A.L., 2001, Hydraulic-property estimates for use with a transient ground-water flow model of the Death Valley regional ground-water flow system, Nevada and California: U.S. Geological Survey Water-Resources Investigations Report 01–4120, 33 p.
- Belcher, W.R., Sweetkind, D.S., and Elliott, P.E., 2002, Probability distributions of hydraulic conductivity for the hydrogeologic units of the Death Valley regional ground-water flow system, Nevada and California: U.S. Geological Survey Water-Resources Investigations Report 02–4212, 24 p.
- Bowen, I.S., 1926, The ratio of heat losses by conduction and by evaporation from any water surface: *Physical Review*, v. 27, p. 779–787.
- Cardinali, J.L., Roach, L.M., Rush, F.E., and Vasey, B.J., 1968, State of Nevada hydrographic areas: Nevada Division of Water Resources map, 1:500,000 scale.
- Carpenter, Everett, 1915, Groundwater in southeastern Nevada: U.S. Geological Survey Water-Supply Paper 365, 86 p., 5 plates.
- Carroll, Rosemary W.H., Giroux, B., Pohll, G., Hershey, R.L., Russell, C.E., and Howcraft, W., 2003, Numerical simulation of groundwater withdrawal at the Nevada Test Site: Las Vegas, University and Community College System of Nevada, Desert Research Institute Publication 45163, 20 p.
- Czarnecki, J.B., 1997, Geohydrology and evapotranspiration at Franklin Lake playa, Inyo County, California, *with a section on* Estimating evapotranspiration using the energy-budget eddy-correlation technique by D.I. Stannard: U.S. Geological Survey Water-Supply Paper 2377, 75 p.

- D'Agnese, F.A., Faunt, C.C., and Turner, A.K., 1998, An estimated potentiometric surface of the Death Valley region, Nevada and California, developed using geographic information system and automated interpolation techniques: U.S. Geological Survey Water-Resources Investigations Report 97-4052, 15 p.
- D'Agnese, F.A., Faunt, C.C., Turner, A.K., and Hill, M.C., 1997, Hydrogeologic evaluation and numerical simulation of the Death Valley regional ground-water flow system, Nevada and California: U.S. Geological Survey Water-Resources Investigations Report 96-4300, 124 p.
- D'Agnese, F.A., O'Brien, G.M., Faunt, C.C., Belcher, W.R., and San Juan, C.A., 2002, A three-dimensional numerical model of predevelopment conditions in the Death Valley regional ground-water flow system, Nevada and California: U.S. Geological Survey Water-Resources Investigations Report 02-4102, 114 p. Accessed September 22, 2004, at <http://pubs.water.usgs.gov/wri024102/>.
- DeMeo, G.A., Laczniak, R.J., Boyd, R.A., Smith, J.L., and Nylund, W.E., 2003, Estimated ground-water discharge by evapotranspiration from Death Valley, California, 1997-2001: U.S. Geological Survey Water-Resources Investigations Report 03-4254, 27 p.
- Dettinger, M.D., 1989, Distribution of carbonate-rock aquifers in southern Nevada and the potential for their development, summary of findings, 1985-88—Program for the study and testing of carbonate-rock aquifers in eastern and southern Nevada, Summary Report No. 1: State of Nevada, Carson City, 37 p.
- Glancy, P.A., 1968, Water-resources appraisal of Mesquite-Ivanpah Valley area, Nevada and California: Nevada Department of Conservation and Natural Resources, Water Resources—Reconnaissance Series Report 46, 57 p.
- Hale, G.S., and Westenburg, C.L., 1995, Selected ground-water data for Yucca Mountain region, southern Nevada and eastern California, calendar year 1993: U.S. Geological Survey Open-File Report 95-0158, 67 p.
- Harrill, J.R., 1986, Ground-water storage depletion in Pah-rump Valley, Nevada-California, 1962-1975: U.S. Geological Survey Water-Supply Paper 2279, 53 p.
- Harrill, J.R., Gates, J.S., and Thomas, J.M., 1988, Major ground-water flow systems in the Great Basin region of Nevada, Utah, and adjacent States: U.S. Geological Survey Hydrologic Investigations Atlas HA-694-C, scale 1:1,000,000.
- Helsel, D.R., and Hirsch, R.M., 1992, Statistical methods in water resources: Amsterdam, Elsevier, 529 p.
- Hevesi, Joseph A., Flint, Alan L., and Flint, Lorraine E., 2002, Preliminary estimates of spatially distributed net infiltration and recharge for the Death Valley region, Nevada-California: U.S. Geological Survey Water-Resources Investigations Report 02-4010, 36 p.
- Hevesi, J.A., Flint, A.L., and Flint, L.E., 2003, Simulation of net infiltration and potential recharge using a distributed-parameter watershed model of the Death Valley Region, Nevada and California: U.S. Geological Survey Water-Resources Investigations Report 03-4090, 161 p.
- Hunt, C.B., Robinson, T.W., Bowles, W.A., and Washburn, A.L., 1966, Hydrologic basin, Death Valley, California: U.S. Geological Survey Professional Paper 494-B, 138 p.
- IT Corporation, 1996a, Underground test area subproject phase I, Data analysis task, volume II—Groundwater recharge and discharge data documentation package: Las Vegas, Nev., Report ITLV/10972-81 prepared for the U.S. Department of Energy, 8 volumes, various pagination.
- IT Corporation, 1996b, Underground test area subproject phase I, Data analysis task, volume IV—Hydraulic parameter data documentation package: Las Vegas, Nev., Report ITLV/10972-81 prepared for the U.S. Department of Energy, 8 volumes, various pagination.
- LaCamera, R.J., and Locke, G.L., 1997, Selected ground-water data for Yucca Mountain region, southern Nevada and eastern California, through December 1996: U.S. Geological Survey Open-File Report 97-821, 79 p.
- LaCamera, R.J., and Westenburg, C.L., 1994, Selected ground-water data for Yucca Mountain region, southern Nevada and eastern California, through December 1992: U.S. Geological Survey Open-File Report 94-54, 161 p.
- LaCamera, R.J., Westenburg, C.L., and Locke, G.L., 1996, Selected ground-water data for Yucca Mountain region, southern Nevada and eastern California, through December 1995: U.S. Geological Survey Open-File Report 96-553, 75 p.
- Laczniak, R.J., DeMeo, G.A., Reiner, S.R., Smith, J.L., and Nylund, W.E., 1999, Estimates of ground-water discharge as determined from measurements of evapotranspiration, Ash Meadows area, Nye County, Nevada: U.S. Geological Survey Water-Resources Investigations Report 99-4079, 70 p.
- Laczniak, R.J., Smith, J. LaRue, Elliott, P.E., DeMeo, G.A., Chatigny, M.A., and Roemer, G.J., 2001, Ground-water discharge determined from estimates of evapotranspiration, Death Valley regional flow system, Nevada and California: U.S. Geological Survey Water-Resources Investigations Report 01-4195, 51 p.

- Lichty, R.W., and McKinley, P.W., 1995, Estimates of ground-water recharge rates for two small basins in central Nevada: U.S. Geological Survey Water-Resources Investigations Report 94-4104, 31 p.
- Malmberg, G.T., 1965, Available water supply of the Las Vegas ground-water basin, Nevada: U.S. Geological Survey Water-Supply Paper 1780, 116 p.
- Malmberg, G.T., 1967, Hydrology of the valley-fill and carbonate-rock reservoirs, Pahrump Valley, Nevada-California: U.S. Geological Survey Water-Supply Paper 1832, 47 p.
- Malmberg, G.T., and Eakin, T.E., 1962, Ground-water appraisal of Sarcobatus Flat and Oasis Valley, Nye and Esmeralda Counties, Nevada: Nevada Department of Conservation and Natural Resources, Ground-Water Resources—Reconnaissance Series Report 10, 39 p.
- Maxey, G.B., and Eakin, T.E., 1950, Ground water in White River Valley, White Pine, Nye, and Lincoln Counties, Nevada: Nevada State Engineer Water Resources Bulletin No. 8, 59 p.
- Maxey, G.B., and Jameson, C.H., 1948, Geology and water resources of Las Vegas, Pahrump, and Indian Springs Valleys, Clark and Nye Counties, Nevada: Nevada State Engineer Water Resources Bulletin no. 5, 43 p.
- Mendenhall, W.C., 1909, Some desert watering places in southeastern California and southern Nevada: U.S. Geological Survey Water-Supply Paper 224, 98 p.
- Miller, G.A., 1977, Appraisal of the water resources of Death Valley, California-Nevada: U.S. Geological Survey Open-File Report 77-728, 68 p.
- Moreo, M.T., Halford, K. J., La Camera, R.J., and Lacznia, R.J., 2003, Estimated ground-water withdrawals from the Death Valley regional flow system, Nevada and California, 1913-98: U.S. Geological Survey Water-Resources Investigations Report 03-4245, 28 p.
- Neuman, S.P., 1982, Statistical characterization of aquifer heterogeneities—An overview, *in* Narasimhan, T.N., ed., Recent trends in hydrogeology: Boulder, Colo., Geological Society of America Special Paper 189, p. 81-102.
- Pistrang, M.A., and Kunkel, F., 1964, A brief geologic and hydrologic reconnaissance of the Furnace Creek Wash area, Death Valley National Monument, California: U.S. Geological Survey Water-Supply Paper 1779-Y, 35 p.
- Reiner, S.R., Lacznia, R.J., DeMeo, G.A., Smith, J.L., Elliott, P.E., Nylund, W.E., and Fridrich, C.J., 2002, Ground-water discharge determined from measurements of evapotranspiration, other available hydrologic components, and shallow water-level changes, Oasis Valley, Nye County, Nevada: U.S. Geological Survey Water-Resources Investigations Report 01-4239, 65 p.
- Rice, W.A., 1984, Preliminary two-dimensional regional hydrologic model of the Nevada Test Site and vicinity: Albuquerque, N. Mex., Sandia National Laboratories Report SAND83-7466, 89 p.
- Rush, F.E., 1968, Water-resources appraisal of Clayton Valley-Stonewall Flat area, Nevada and California: Nevada Department of Conservation and Natural Resources, Water Resources—Reconnaissance Series Report 45, 54 p.
- Rush, F.E., 1970, Regional ground-water systems in the Nevada Test Site area, Nye, Lincoln, and Clark Counties, Nevada: Carson City, Nevada Department of Conservation and Natural Resources, Ground-Water Resources—Reconnaissance Series Report 54, 25 p.
- Russell, C.E., and Minor, T., 2002, Reconnaissance estimates of recharge based on an elevation-dependent chloride mass balance approach: Las Vegas, University and Community College System of Nevada, Desert Research Institute Publication 45164, 57 p.
- Stonstrom, D.A., Prudic, D.E., Lacznia, R.L., Akstin, K.C., Boyd, R.A., and Henkelman, K.K., 2003, Estimates of deep percolation beneath native vegetation, irrigated fields, and the Amargosa River channel, Amargosa Desert, Nye County, Nevada: U.S. Geological Survey Open-File Report 03-104, 83 p.
- U.S. Department of Agriculture, 1994, State Soil Geographic (STATSGO) Data Base—Data use information: U.S. Department of Agriculture Miscellaneous Publication no. 1492.
- Van Denburgh, A.S., and Rush, F.E., 1974, Water-resources appraisal of Railroad and Penoyer Valleys, east-central Nevada: Nevada Department of Conservation and Natural Resources, Water Resources—Reconnaissance Series Report 60, 61 p.
- Waddell, R.K., 1982, Two-dimensional, steady-state model of ground-water flow, Nevada Test Site and vicinity, Nevada-California: U.S. Geological Survey Water-Resources Investigations Report 82-4085, 72 p.
- Walker, G.E., and Eakin, T.E., 1963, Geology and ground water of Amargosa Desert, Nevada-California: Nevada Department of Conservation and Natural Resources, Ground-Water Resources—Reconnaissance Series Report 14, 45 p.

- Waring, G.A., 1915, Springs of California: U.S. Geological Survey Water-Supply Paper 338, 410 p.
- Waring, G.A., revised by Blankenship, R.R., and Bentall, Ray, 1965, Thermal springs of the United States and other countries of the world—A summary: U.S. Geological Survey Professional Paper 492, 383 p.
- West, N.E., 1988, Intermountain deserts, shrub steppes, woodlands, *in* Barbour, M.G., and Billings, W.D., eds., North American terrestrial vegetation: Cambridge, Cambridge University Press, 434 p.
- Westenburg, C.L., and LaCamera, R.J., 1996, Selected groundwater data for Yucca Mountain region, southern Nevada and eastern California, through December 1994: U.S. Geological Survey Open-File Report 96-205, 73 p.
- Winograd, I.J., and Thordarson, William, 1975, Hydrologic and hydrochemical framework, south-central Great Basin, Nevada-California, with special reference to the Nevada Test Site: U.S. Geological Survey Professional Paper 712C, p. C1-C126.